ST. ANTHONY FALLS HYDRAULIC LABORATORY
UNIVERSITY OF MINNESOTA

Project Report No. 61

TANDEM INTERFERENCE EFFECTS OF FLAT NONCAVITATING HYDROFOILS

Submitted by
LORENZ G. STRAUB
Director

Prepared by
J. M. WETZEL and W. H. C. MAXWELL

May 1962

Prepared for
BUREAU OF SHIPS
Department of the Navy
Washington, D.C.
under
Bureau of Ships Project No. SF 013 02 01, Task 1702
Office of Naval Research Contract Nonr 710(41)

PREFACE

The use of hydrofoils in a tandem configuration results in an interference problem somewhat similar to the wing-tail problem encountered in aerodynamics. However, the presence of a free surface and the surface waves generated by the foil modify the methods of analysis. The studies described in this report were initiated to obtain experimental information on the interference or downwash effect of two identical noncavitating hydrofoils in tandem for smooth water conditions. Limited tests were also conducted in a progressive wave train.

The study was carried out in the period November 1, 1960 to May 31, 1962, under terms of Office of Naval Research Contract Number Nonr 710(41), Bureau of Ships Project Number SF 013 02 01, Task 1702.

The report was critically reviewed by C. E. Bowers. The assistance of F. R. Schiebe and F. Thomas is gratefully acknowledged. Special acknowledgement is given to Wallace H. Parmenter, who was primarily responsible for the design of the experimental apparatus as well as securing most of the experimental data. The report was prepared for publication by Marjorie Olson and Carol Takyi under the general supervision of Loyal Johnson.

A B S T R A C T

Experimental measurements were made of the interference effect of two submerged, flat, noncavitating hydrofoils of finite span in tandem. The surface wave generated by a single foil was measured in the longitudinal and lateral directions. Downwash angles were determined from the experimental data for various foil separations and submergences. Comparison of the results with theory was favorable. Limited measurements were also made of the oscillatory lift and drag forces for a foil moving through a progressive wave train. The data agreed with quasi-steady theory for the lower frequencies of encounter. At the higher frequencies of encounter, consideration of unsteadiness effects improved the correlation.

C O N T E N T S

LIST OF ILLUSTRATIONS

LIST OF SYMBOLS

a - Wave amplitude.

b - Semi-span of rear foil in tandem system.

C_D - $2D/\rho SV^2$, drag force coefficient.

$C_{D_{strut}}$ - $2\ D_{strut}/\rho SV^2$, strut drag force coefficient.

C_L - $2L/\rho SV^2$, lift force coefficient.

c - Hydrofoil chord.

c_w - Wave celerity.

d - Water depth.

f - Submergence of foil below undisturbed surface.

g - Acceleration due to gravity.

i - $\sqrt{-1}$.

$J_n(z)$ - Bessel function of first kind of order n and argument z.

K - $K_o \sec^2 \theta \tanh Kd$, wave number in shallow water.

K_o - g/V^2, wave number.

Re - Real part of a complex quantity.

S - Hydrofoil planform area.

s - Semi-span of Hydrofoil.

t - Time.

u - Horizontal component of orbital velocity in a wave.

V - Forward speed of hydrofoil.

w - Vertical component of orbital velocity in a wave.

x, y, z - Co-ordinates of any point in the fluid measured from a right-handed set of axes whose origin is in the plane of the undisturbed free surface and directly above the foil lifting line. Positive z is directed upward (in two-dimensional theory, the co-ordinate z is absent and the vertical co-ordinate is y, directed positive upward).

α - The geometric angle of attack.

ϵ - Downwash angle, taken as positive when it causes a reduction in the angle of attack.

ζ - Surface wave elevation due to foil.

η - Regular progressive surface wave elevation.

θ - Wave direction angle measured from fore-and-aft direction to the normal to a wave element.

λ - Wave length.

ν - Frequency of encounter: $(2\pi/\lambda)(V + c_w)$ in head seas,
$(2\pi/\lambda)(V - c_w)$ in following seas.

ρ - Fluid density.

ϕ_D - Drag phase lead.

ϕ_L - Lift phase lead.

Subscript f, a - Indicate forward or aft foil.

Subscript s - Indicates smooth water value.

Subscript w - Indicates component due to progressive wave.

TANDEM INTERFERENCE EFFECTS OF FLAT, NONCAVITATING HYDROFOILS

I. INTRODUCTION

In the design of hydrofoil craft, more or less standard aerodynamic techniques are used whenever possible to make most efficient use of the vast storehouse of information accumulated throughout many years. However, in the case of hydrofoils operating near the free water surface, the flexible boundary introduces effects that have no precedent in the aerodynamic field. Aside from the fact that the presence of the free surface results in a reduction of the lift force, a stationary wave train is also created behind the foil. The energy to maintain this wave train is provided by the foil and therefore an additional drag or resistance is observed. This additional drag, commonly called wave drag, diminishes as the speed of the foil increases. In an attempt to obtain information concerning these additional effects, a number of theories [1, 2, 3, 4, 5, 6, 7]* has been developed to permit calculation of the forces on a foil near a free surface. The components of the drag determined by the potential theory are restricted to the wave drag and the induced drag, the latter being of importance for a foil of finite span. As a typical hydrofoil craft uses at least two foils in the interest of obtaining longitudinal stability, the associated interference effect created by the forward foil is of considerable importance. As the wave train generated by the forward foil moves at the same speed as the foil, it is possible for the aft foil to be placed in regions of minimum or even negative downwash (upwash) with a resultant increase in the performance of the aft foil. This possibility has stimulated rather extensive theoretical work in this area.

The theoretical developments that are useful in this paper are those for a hydrofoil of finite span. The principal theoretical work for this case is described in References [2] and [3]. The effect of the finite span is to change the pattern of waves generated by the foil, as waves are also created by the foil tips. The wave drag is considerably different, particularly for speeds near the critical Froude number. It has been previously shown that

---

*Numbers in brackets refer to the List of References on p. 15.

for a two-dimensional foil the wave drag should be zero for all values of the depth Froude number greater than one. The result is somewhat unrealistic to apply to a foil of finite span, as the lateral wave system generated by the tips can contain waves whose velocity is less than critical and thus can carry energy away from the foil. Earlier work has also indicated that the pattern of the waves and therefore the wave drag is dependent upon the depth of water in the towing tank. It is generally considered that for velocities greater than about 0.6 the critical velocity, the water depth will have considerable influence on the wave characteristics. In this respect, Breslin [3] has developed a theory to account for the finite depth, and some computations made using this theory are included in another section.

In the current investigations, the items of particular interest were the surface waves generated by a foil near the free surface, and the downwash effect of the forward foil on the aft foil of a tandem configuration. Kaplan et al. [2] have developed a theory specifically for these particular cases, and this theory has therefore been used for many of the computations. The theory was formulated for a hydrofoil at a finite submergence moving through fluid of infinite depth. The computations based on any complete theory were somewhat lengthy, as a numerical computation of several integrals was required for both the profile of surface wave and the downwash angle. The equations used in the comparison with experimental data are summarized in the Appendix. The effect of the upwash pattern ahead of the aft foil on the forward foil of a tandem system and the effect of the upwash on the free surface ahead of the forward foil were neglected. The effect of roll-up of the tip vortices from the rear foil on the spanwise distribution of downwash across the rear foil was also neglected and only the average downwash at the rear foil considered, both in the theoretical treatment and in the experimental measurements. For design purposes it would be advantageous to obtain more theoretical and experimental information on the spanwise distribution of the downwash in the vicinity of the rear foil. The rear foil behaves essentially as a twisted foil in view of the variation of effective angle of attack across its span. It is probable that at a particular location at which downwash occurs over the major part of the span of an aft foil a region of upwash occurs near its tips because of the roll-up of the tip vortices emanating from the forward foil.

A limited experimental verification of theory has previously been made concerning the tandem interference effect, although no systematic tests appear to have been conducted or published in the unclassified literature. To obtain more information in this area, the tests described in the present report were initiated. Some measurements of the oscillatory lift and drag forces for a flat hydrofoil moving through a progressive wave train are also reported. The work was sponsored by the Office of Naval Research, under contract Nonr 710(41).

II. EXPERIMENTAL APPARATUS AND PROCEDURE

A. Towing Facility

The tests were conducted in the Laboratory towing facility. The tank had a length of 220 ft, width of 9 ft, and a depth of 6 ft, and was filled with water to a depth of 4.5 ft. The self-propelled towing carriage was capable of attaining speeds up to 25 fps, although the speed for this particular study was limited to 20 fps to allow a sufficient time for transient effects to become insignificant. The tank was also equipped with a paddle-type wave generator capable of generating waves from 2 ft to 40 ft in length. The steepest wave that can be generated is about 17 ft long and 2 ft high. A sloping permeable beach absorber was located at the opposite end of the tank to minimize reflections of the generated wave.

B. Foils and Instrumentation

Two identical hydrofoils of zero dihedral angle and rectangular planform were used for all the tests in the program. The foils were machined from aluminum to a NACA 16-509 section. This section has a rather uniform pressure distribution and is therefore very well suited for practical applications. Each of the foils had a 3-in. chord and an 18-in. span (aspect ratio = 6), and was attached to a strut of 3-in. chord and NACA 16-012 section. The single strut was attached to the hydrofoil at mid-span. One of the strut-foil assemblies was attached to a two-component strain-gage dynamometer to permit measurement of lift and drag forces. The lift and drag were measured perpendicular and parallel to the direction of motion, respectively, as shown in Fig. 1. The natural frequency of the dynamometer, foil, and support mechanism was

25 cps in the lift direction. As the largest frequency of encounter was about 6 cps, errors of less than about 5 degrees in phase and 5 per cent in amplitude were introduced by the dynamometer itself at a maximum damping of 0.13 critical. A four-channel Sanborn recorder was used to obtain a continuous record of the force characteristics. It was also possible to vary the submergence, f, angle of attack, α, and in the case of tandem tests the separation of the foils, x. The angle of attack was taken to be the geometric angle, and the submergence was measured from the still water surface to the leading edge of the foil.

The profile of the wave train created by a single foil moving through otherwise smooth water was measured with a sonic wave transducer for a number of conditions. The transducer used for this phase of the program is described in Reference [8]. The sonic head of the transducer was mounted on a subcarriage attached to temporary rails on the underside of the main towing carriage. The subcarriage was designed to permit traversing the wave profile both in the longitudinal and lateral directions. When measuring the profile in the longitudinal direction, the sonic head was rigidly fastened to the subcarriage at a particular spanwise distance from the center of the foil, and the entire subcarriage was moved manually with respect to the main carriage. For measuring the profile in the transverse or lateral direction, the subcarriage was fixed at a given distance downstream of the foil, and the sonic head was moved laterally on the subcarriage. The instantaneous position of the subcarriage or the sonic head itself was determined through potentiometers attached to the subcarriage wheels. The outputs of these potentiometers were fed into the X input of a Mosley XY recorder. The sonic head output was fed into the Y input of the recorder. This arrangement made it possible to obtain the wave profile independently of the speed at which the subcarriage was moved. Static measurements of the still water surface indicated that depressions of less than 1/16 in. could be measured, thus giving considerable confidence in the accuracy of the instrument for work of this nature.

C. Procedure

Lift and drag measurements were made for a single foil in smooth water for velocities of 5, 10, 15, and 20 fps. The geometric angle of attack was varied from -4 to 12 degrees, and the submergence from 1 to 3 chords. Values of the submergence Froude number varied from 1 to 7, and the chord

Reynolds number varied from about 1.25×10^5 to 5×10^5. Measurements of the longitudinal wave profile at the center of the span were made for several velocities, submergences, and angles of attack. In some cases, the wave profile was also measured at a number of spanwise locations to obtain a more complete mapping and to determine the disturbance effect of the center strut on the wave train.

For the tandem tests, the aft foil was attached to a device that could be moved in the longitudinal direction to readily vary the separation of the foils. Both foils were placed at a given angle of attack and submergence, and the horizontal and vertical components of the forces were measured by the dynamometer on the aft foil for given velocities and separations of the foils.

Brief tests were also conducted to determine the oscillatory lift and drag forces for foils moving through a regular wave train, both in head and following seas. Wave lengths from 3 to 10 ft were used for these tests, with peak-to-peak amplitudes varying from 0.05 to 0.30 ft. The submergence and geometric angle of attack were maintained at 1 chord and 4 degrees, respectively, for all the tests. For a few limited conditions, force measurements were also made on the aft foil of a tandem configuration moving through regular waves.

III. DISCUSSION OF RESULTS

A. Force Data for Single Foil in Smooth Water

The forces were measured on a single foil in smooth water for various angles of attack, submergences, and towing velocities to serve as a reference when the foils were placed in a tandem configuration. The data, reduced in terms of the standard force coefficients, are shown in Fig. 2. The coefficients in all cases were based on the planform area of the foil. The solid line shown on the lift coefficient plots was calculated from the semi-empirical equation presented by Tinney [9],

$$C_L = \frac{C_{L_2}}{1 + \frac{2}{AR}} \left[1 - 0.422e^{-1.454\, f/c}\right] \qquad (1)$$

where C_{L_2} = two-dimensional coefficient from airfoil data,
AR = aspect ratio, span/chord for rectangular planform, and
f/c = submergence in chords.

Several discrepancies can be noted in this comparison. The angle of zero lift is somewhat greater than that generally found for airfoils. The angle decreases with increasing velocity. This is in agreement with other data described by Breslin [3] where a strong dependence on span Froude number, $V/\sqrt{2gs}$, has been noted up to values of 1.7. In the present tests with a span of 1.5 ft, this Froude number would correspond to a velocity of 11.8 fps. The data in Fig. 2 indicate that no dependence on velocity exists for speeds above 15 fps, although this independence may occur at some lower velocity between 10 and 15 fps as well. The disagreement between the asymtotic value and airfoil value may have been caused by an error in setting of the reference angle of attack. This was not considered serious, as the lift curve slope was of considerably greater importance than the absolute angle of attack.

The measured lift curve slope was generally the same as that calculated for angles less than about 4 degrees. Theory by Nishiyama [5] indicates that Eq. (1) underestimates the lift on a flat foil of aspect ratio 8- and 2-chord submergence for submergence Froude numbers from about 1 to 4. The submergence Froude numbers for this investigation varied from about 1 to 7.

The total drag on a submerged foil can be considered to be the sum of several components: strut, profile, induced, and wave drags. The induced and wave drags are known to be functions of the square of the lift coefficient. Total drag coefficients as a function of the angle of attack are also shown in Fig. 2. In these plots, the drag of the strut has also been included, which accounts for some of the change in drag coefficient with submergence. The drag coefficient becomes smaller at the higher velocities, primarily through the reduction of the wave drag component with increasing velocity.

Drag measurements of the strut alone were also made, and the drag was subtracted from the total drags previously shown in Fig. 2 to obtain the net drag on the foil. Plots of the force coefficients are shown in Fig. 3 as polar diagrams; in this case the strut drag has been subtracted from the total drag. At the lower velocity, the effect of submergence is quite large, whereas, as the velocity increases, the submergence effect diminishes. Data for velocities of 15 and 20 fps are shown in Fig. 3c. A comparison of data

with that presented in Reference [10] for a velocity of 20 fps, and 1-chord submergence is also shown in Fig. 3c. Good agreement was obtained for this velocity, and as the tests described in [10] were conducted at velocities of 20 fps and above, no further overlap in data between the two sources was possible.

The slope of a straight line drawn through the origin and tangent to the curves in the polar diagram represents the maximum performance ratio (lift/drag) for the particular velocity and submergence. The angle of attack for the maximum ratio was generally about 4 degrees. Assuming that the maximum performance would be of most interest in the prototype, this angle was used for the majority of the tests with foils in tandem.

The variation of measured strut drag with velocity, submergence, and angle of attack is shown in Fig. 3d. The strut drag coefficients as plotted were based on the area of the foil, rather than the submerged area of the strut. The strut drag increases quite rapidly with decreasing velocity. Little difference in strut drag was noted for angles of zero and 4 degrees, but the drag increased at 8 degrees, particularly for the lower velocity. The slashes on the data points are used to identify the data points for each particular submergence.

B. Surface Waves Generated by Single Foil

As a body approaches the free water surface, waves that are stationary with respect to the body are generated on the surface. In the case of a flat hydrofoil of finite span, waves are also created by the tips of the foil, and the resulting wave pattern attains a more complicated form. The aft foil of a hydrofoil system is usually placed in the wave created by the forward foil. This wave will thus change the characteristics of the flow about the aft foil and result in different force distributions.

The resultant force on the aft foil is altered essentially through the change in angle of attack created by the vertical component of the orbital velocity of the wave. The maximum change therefore occurs at the midpoint between crest and trough, or trough and crest. At the crest or trough the orbital velocity vector is horizontal, with no resultant change in the angle of attack. The orbital velocity is attenuated with distance from the smooth water surface in an exponential manner. Several theories, References [2, 3],

have been developed to predict the shape of the stationary wave for foils of finite span. The final results of these theories are presented in the Appendix for reference purposes.

Typical longitudinal wave profiles at the centerline of the span for various submergences and velocities of the foil are shown in Figs. 4 and 5. These profiles were traced directly from the plots obtained from the XY recorder. It can be noted that for a given submergence the period of the wave increases with the velocity. As the submergence of the foil increases, the wave amplitude decreases, and the points of maximum or minimum amplitude change slightly. It was not possible to measure the wave profile closer to the foil than about 6 chords, because of limitations in the experimental apparatus. This was not considered undesirable as the theory used for comparison with the data also was not valid in regions close to the foil. The wave profile was also calculated for a submergence of 2 chords and a $V = 15$ fps from Eq. (A-3) in the Appendix and is shown by the dashed line in Fig. 4. The agreement between theory and experiment is fairly good, both with respect to wave amplitude and oscillatory trends. As most interest was in the downwash calculations, extensive computations were not carried out for the wave profile.

The wave profiles generated by the foil at a larger angle of attack are shown in Fig. 5. According to Eq. (A-3), the wave amplitude should increase linearly with the lift coefficient. A comparison of Figs. 4 and 5 will reveal that this is generally the case, particularly for the lower velocities and smaller submergences. Points of maximum and minimum amplitude remain relatively unchanged.

For one particular condition, measurements of the longitudinal profiles were also made at various positions in a spanwise direction along the foil. These profiles are shown in Fig. 6 for a velocity of 5 fps and submergence of 1 chord. The ordinate on the right of the plot indicates the spanwise position of the measuring station, and the left ordinate indicates the wave elevation for each particular station. The scale for the wave elevation is indicated in the lower left corner of the graph. The center of the span is at $y/s = 0$, and the outboard tip of the foil is at the point $y/s = 1$. As the foil and the resulting wave pattern were symmetrical, only one half of the pattern is shown. The broken lines were roughly sketched through the crest and trough of the waves. As the distance from the centerline of the

foil, y, increases the wave crests tend to bend aft due to effects of the finite span. Little difference has been observed in the wave profiles taken at the centerline and at small transverse distances from the centerline, thus indicating minor interference by the strut.

C. Tandem Foils in Smooth Water

1. Force Coefficients

Figures 7, 8, and 9 show results for force coefficients of the aft foil for various velocities and submergences of the forward and aft foils. In all of these plots, it can be noted that the oscillation of the coefficients is greatest for the lowest velocity. This is directly associated with the wave pattern generated by the foil. Also, for a given submergence of the forward foil, the amplitude of the forces becomes less with increasing submergence of the aft foil, indicating that the interference effect is attenuated. Furthermore, it is also interesting to note that at a foil separation where the measured lift is a maximum, a comparison with the associated drag plot shows that the measured drag is near a minimum. For example, in Fig. 7 for a velocity of 5 fps, submergence of 1 chord, and a foil separation of 8 chords, the lift and drag are essentially maximum and minimum. The solid line in these figures represents the wave profiles taken from Fig. 4 and is replotted to relate the position of the stationary wave to the force coefficients. Only one profile has been presented as it has been previously shown that submergence had little effect on the oscillatory trends. Thus, the maximum lift and minimum drag (maximum performance ratio) occur near the point of maximum upwash. The location of this point varies slightly with submergence, but more strongly with velocity, as the length or period of the stationary wave necessarily changes with velocity.

The increase in lift and decrease in drag may be explained in the following manner. The lift and drag forces were measured in directions perpendicular and parallel to the direction of motion (horizontal) at all times. As the foil moved into a region of upwash, the true lift and drag (referred to the instantaneous velocity vector) both increased. However, the resultant force vector was tipped forward of its original position, resulting in a decrease in the indicated or measured drag. If the instantaneous angle was of sufficient magnitude to rotate the force vector forward of the vertical, a

negative drag would be measured. For the foil moving through a downwash region the reverse was true, in that the measured lift decreased and the measured drag increased. The above explanation is valid only for a fully wetted flow. This relationship is also significant in the determination of phase relationships for a foil moving through a progressive wave train and will be discussed in a later section.

2. Downwash Angle

The average downwash angle was determined by measuring the lift coefficient on the aft foil at various horizontal and vertical distances from the forward foil. The downwash angle was then calculated by using the angle of attack for a single foil that would give the same lift coefficient in still water as that measured on the aft foil of the tandem system. The difference between the geometrical angle of attack and this angle was then taken as the downwash angle. The downwash angle was considered positive when it tended to reduce the lift on the foil, thus corresponding to the downwash angle in the usual aerodynamic sense.

The theoretical downwash angle was determined for several conditions using two-dimensional theory and three-dimensional theory for a fluid of infinite depth from Reference [2]. The equations used for these computations are included in the Appendix. The computations were limited in scope as the numerical integrations were quite lengthy. A comparison of the various theories, as well as a comparison with experimental data, is shown in Fig. 10a for a velocity of 5 fps and the forward and aft foils at 2-chord submergences. The downwash angle in degrees has been divided by the lift coefficient of the forward foil. One of the curves shown is empirical and was based on experimental data from Reference [11] for a foil with an aspect ratio of 20 at a submergence of 1 chord. It is included on this plot to indicate the difference between the two-dimensional theory by Kaplan and the empirical curve for a foil of very high aspect ratio. The three-dimensional theory for an aspect ratio of 6 (Eq. (A-5)) exhibits a somewhat constant value of downwash that appears to be slightly higher than that determined from the experimental data. Points of maximum and minimum downwash are predicted quite well by both the two- and three-dimensional theories. The measured amplitude of downwash oscillation is somewhat greater than calculated for the finite span foil.

Additional comparisons of the three-dimensional theory and data are shown in Figs. 10b and 10c for velocities of 10 and 15 fps. The correlation tends to be considerably improved as the velocity increases, particularly for the larger distances aft of the leading edge. Since the theoretical curves calculated from Eqs. (A-5) and (A-6) were almost co-incident, even at a velocity of 5 fps, only one of the curves has been shown for the sake of clarity.

It should be mentioned that the accuracy of the experimental data for the downwash angle depended rather strongly on the lift curve slope. Furthermore, the method of plotting tends to exaggerate the errors at this scale since the lift coefficient of the forward foil was always less than one.

Several tests were also made to determine the relationship between downwash angle and angle of attack (lift coefficient) of the forward foil. The results of these tests for velocities of 5, 10, and 15 fps and two foil separations are shown in Fig. 11. The separations of 8 and 16 chords were selected to give maximum values of the downwash at the lower velocity. It can be seen that the downwash angle varies linearly with the angle of attack, the slope, $d\epsilon/\partial\alpha$, depending on the velocity and the distance from the forward foil. This is of course related to the change in the stationary wave pattern with velocity as previously seen in Figs. 4 and 5.

As it has been shown that the relationship between downwash and lift was essentially linear, most tests to determine the downwash angle were therefore conducted at one angle of attack of the forward foil. The results of these tests are plotted in Figs. 12 and 13 for various velocities and submergences. For the data in each of the figures the submergence of the forward foil, f_f, was held constant and the submergence of the aft foil, f_a, varied as indicated by the ratio f_a/f_f. The wave profile taken from Fig. 4 is also included for reference purposes. The elevation of the wave at any point is given by the ordinate at the right of the plot. Again the downwash angle has been divided by the lift coefficient of the forward foil. The attenuation of the downwash angle as the aft foil increases in submergence from 1 to 3 chords is generally apparent. Also, the maximum or minimum effects are noted to occur at the position in the surface wave generated by the forward foil that represents extreme values of the vertical component of orbital velocity. For example, from Fig. 12 for $V = 5$ fps, for a foil separation of about 18 chords, the maximum downwash can be seen to occur in the region at which the vertical

component of orbital velocity is maximum. In some cases a slight lag is observed.

D. Oscillatory Forces

Measurements were made of the oscillatory lift and drag forces for a restrained foil moving through regular head and following seas. All of the measurements were made with a submergence of 1 chord and an angle of attack of 4 degrees. Typical data concerning the maximum change in the lift coefficient in head seas is shown in Fig. 14 for three velocities and three wave heights (2a). The reduced frequency, $\nu c/2V$, is a measure of the unsteadiness and for these conditions varied from about 0.07 to 0.23. Calculated curves are shown using quasi-steady linear theory given by Eq. (A-9) and unsteady linear theory, Eq. (A-11), for a velocity of 10 fps. It can be seen that in general the quasi-steady theory tends to overestimate the effect of the wave on the forces, particularly for the larger wave amplitude. A rather large discrepancy appears to exist for a wave height of 0.2 ft for all three velocities. In checking the raw data, no error could be found in the experimental points. The solid symbols represent data taken for the aft foil in a tandem configuration at velocities of 10 and 15 fps. The forward foil was set at a 1-chord submergence and angle of attack of 4 degrees, and the two foils were separated a distance of 8 chords. The entire configuration was then towed through regular waves. It can be noted that little difference in the lift coefficient was found between the single foil and the aft foil in tandem. Referring back to Fig. 12 for tandem foils in smooth water, a considerable downwash effect existed at a separation of 8 chords, resulting in a substantial change in the lift coefficient. It is possible that the progressive wave train disrupted the stationary train to the extent that no appreciable effect could be noticed.

Measurements in following seas were limited to one towing velocity. The lift data are shown in the bottom graph of Fig. 14 for a peak-to-peak amplitude of 0.30 ft. The quasi-steady theory agrees rather well for this case. As the reduced frequency varies from about 0.08 to 0.018, the unsteadiness effects would be expected to be small.

In general, the measurements of the oscillatory drag forces were difficult to obtain with satisfactory accuracy. Drag data for a towing velocity of 5 fps were of such poor quality that they are not presented. Data for

the maximum oscillatory drag coefficient at the higher velocities are shown in Fig. 15. The data are compared with the quasi-steady theory given by Eq. (A-10). The calculations include the fundamental only, although the amplitude of the second harmonic component may be rather large. However, the test records of the experimental drag exhibited considerable harmonic distortion as well. In most cases it appeared that a strong second harmonic was present. Time and funds did not permit a detailed harmonic analysis of the records, and a rough estimate was made as to the magnitude of the maximum drag amplitude.

Some results of the phase relationships between the forces and the waves are also shown in Fig. 15. The phase was defined as the number of degrees of wave cycle that the maximum forces taken in a positive direction led the wave crest. Only the quasi-steady values for the fundamental were calculated for comparison with data. Again, it will be noted that the data for following seas agree more favorably with theory. The experimental data for phase relationships were not available for every test run due to difficulty in obtaining satisfactory records. This was particularly true for the drag phase relationship. The data points shown were based directly on the trace on the experimental record. The harmonic distortion present in most cases would alter the values somewhat from those shown. However, visual inspection of the test records in most cases indicated that the lift and drag forces were approximately 180 degrees out of phase with each other. Only with the foil placed at an extremely high angle of attack, about 12 degrees, could this phase relationship be changed by any significant amount.

IV. CONCLUSIONS

The results of the investigation for fully wetted, noncavitating foils may be summarized as follows:

(1) The surface wave profile created by a foil near the free surface can be satisfactorily predicted by three-dimensional theory from Reference [2].

(2) The performance characteristics of the aft foil in a tandem configuration can be improved by placing the foil in the region of maximum upwash.

(3) Comparisons of calculated average downwash angles from Reference [2] and angles based on experiment indicated favorable agreement, particularly for the high velocities and large distances aft of the forward foil. The downwash angle was essentially a linear function of the lift coefficient.

(4) Measurements of the additional lift created by a foil moving through a progressive wave train have shown that the quasi-steady theory overestimates the additional lift in head seas and larger wave amplitudes. The agreement improves for smaller amplitudes and also for following seas or lower reduced frequencies, $\nu c/2V$.

(5) The experimental phase relationship between the lift and drag appears to be about 180 degrees, regardless of the direction of the progressive wave train. Qualitative comparison between quasi-steady theory and phase with respect to the wave has been obtained, although additional data for the oscillatory drag would be desirable.

LIST OF REFERENCES

[1] Wu, Y. T. "A Theory for Hydrofoils of Finite Span," Journal of Mathematics and Physics, Vol. 33, pp. 207-248. October 1954.

[2] Kaplan, P., Breslin, J. P. and Jacobs, W. R. Evaluation of the Theory for the Flow Pattern of a Hydrofoil of Finite Span. Stevens Institute of Technology, Experimental Towing Tank Report 561. May 1955.

[3] Breslin, J. P. "The Wave and Induced Drag of a Hydrofoil of Finite Span in Water of Limited Depth," Journal of Ship Research, Vol. 5, No. 2, pp. 15-21. September 1961.

[4] Nishiyama, Tetsuo. "Lifting-Line Theory of the Submerged Hydrofoil of Finite Span, Part I," American Society of Naval Engineers Journal, Vol. 71, No. 3, pp. 511-519. August 1959.

[5] Nishiyama, Tetsuo. "Lifting-Line Theory of the Submerged Hydrofoil of Finite Span, Part II," American Society of Naval Engineers Journal, Vol. 71, No. 4, pp. 693-700. November 1959.

[6] Nishiyama, Tetsuo. "Hydrodynamical Investigation on the Submerged Hydrofoil, Part III," American Society of Naval Engineers Journal, Vol. 71, No. 1, pp. 135-142. February 1959.

[7] Isay, W. H. "Zur Theorie der Nahe der Wasseroberflache Fahrenden Tragflachen," Ingenieur-Archiv, Vol. 27, No. 5, pp. 295-313. 1960.

[8] Killen, John M. The Sonic Surface-Wave Transducer. University of Minnesota, St. Anthony Falls Hydraulic Laboratory Technical Paper No. 23, Series B. July 1959.

[9] Tinney, E. Roy. Experimental and Analytical Studies of Dihedral Hydrofoils. University of Minnesota, St. Anthony Falls Hydraulic Laboratory Project Report No. 41. November 1954. (Not available for distribution)

[10] Wadlin, Kenneth L., Shuford, Charles L. Jr., and McGehee, John R. A Theoretical and Experimental Investigation of the Lift and Drag Characteristics of Hydrofoils at Subcritical and Supercritical Speeds. NACA Report 1232. 1955.

[11] Breslin, John P. An Investigation of the Characteristics of the Waves Produced by a Hydrofoil. ONR Hydrofoil Research Project, Bath Irons Works Corporation by Gibbs and Cox Inc., Technical Report No. 13. May 1953.

[12] Kaplan, Paul. The Forces and Moments Acting on a Tandem Hydrofoil System in Waves. Stevens Institute of Technology, Experimental Towing Tank Report No. 506. December 1955.

F I G U R E S

(1 through 15)

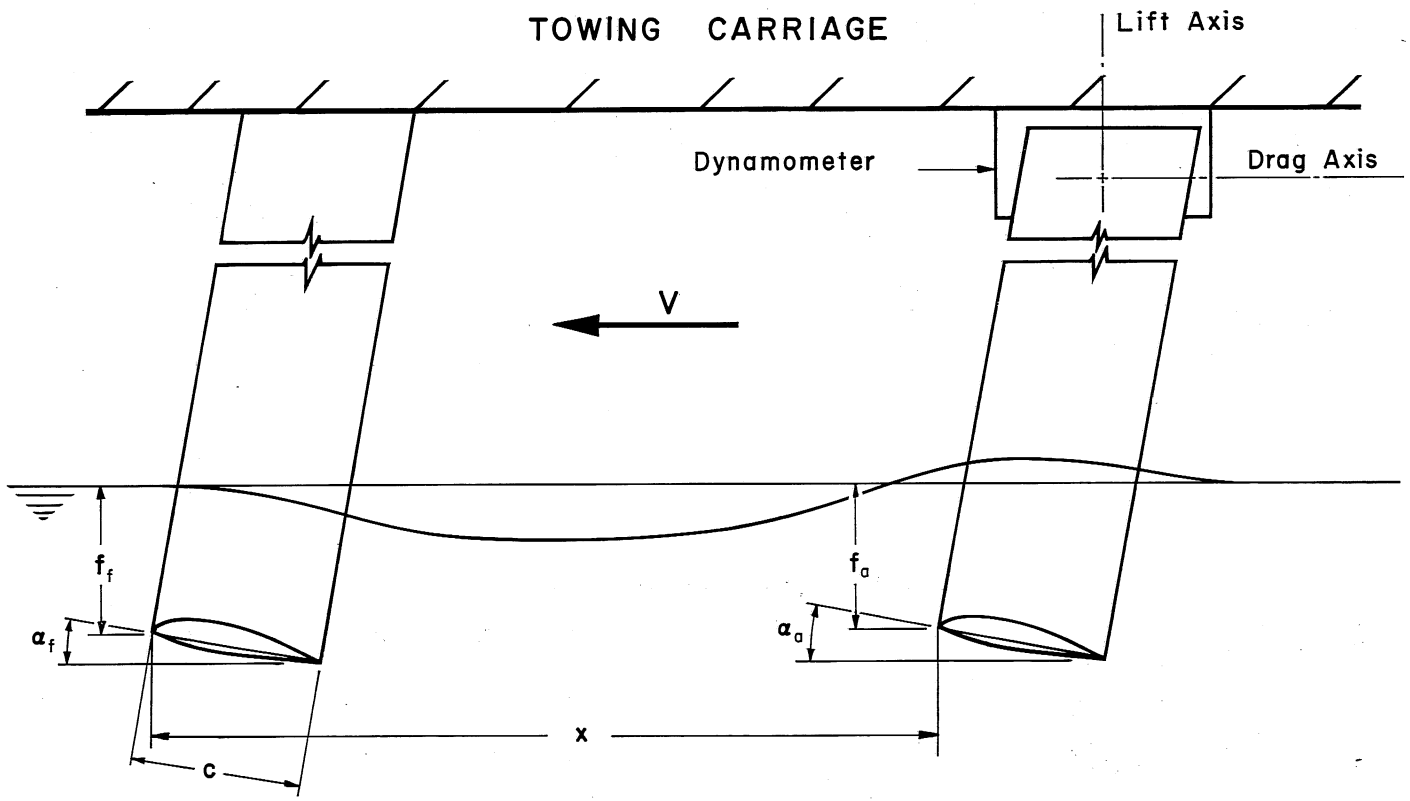

Fig. 1 – Definition Sketch

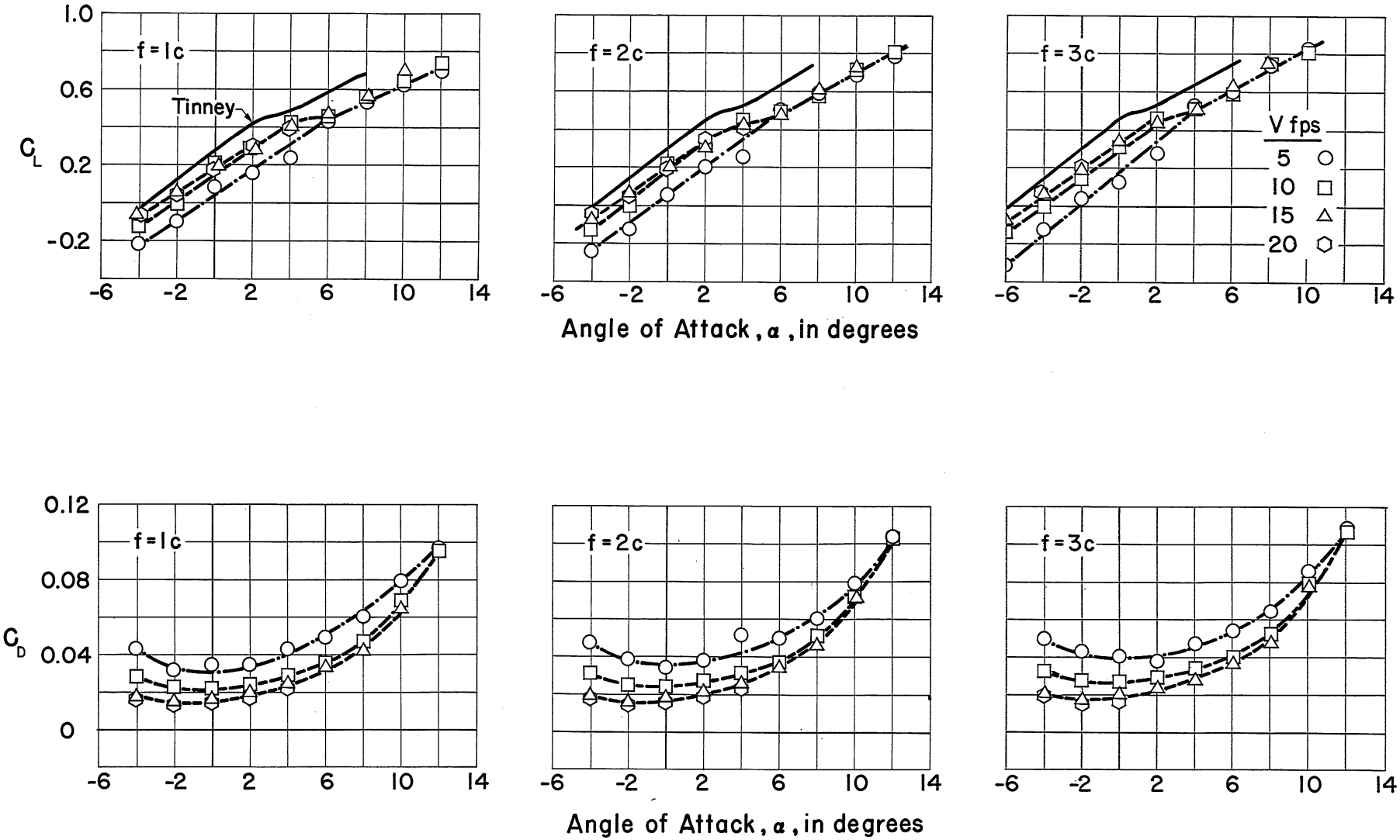

Fig. 2 – Force Coefficients for Single Foil---Smooth Water

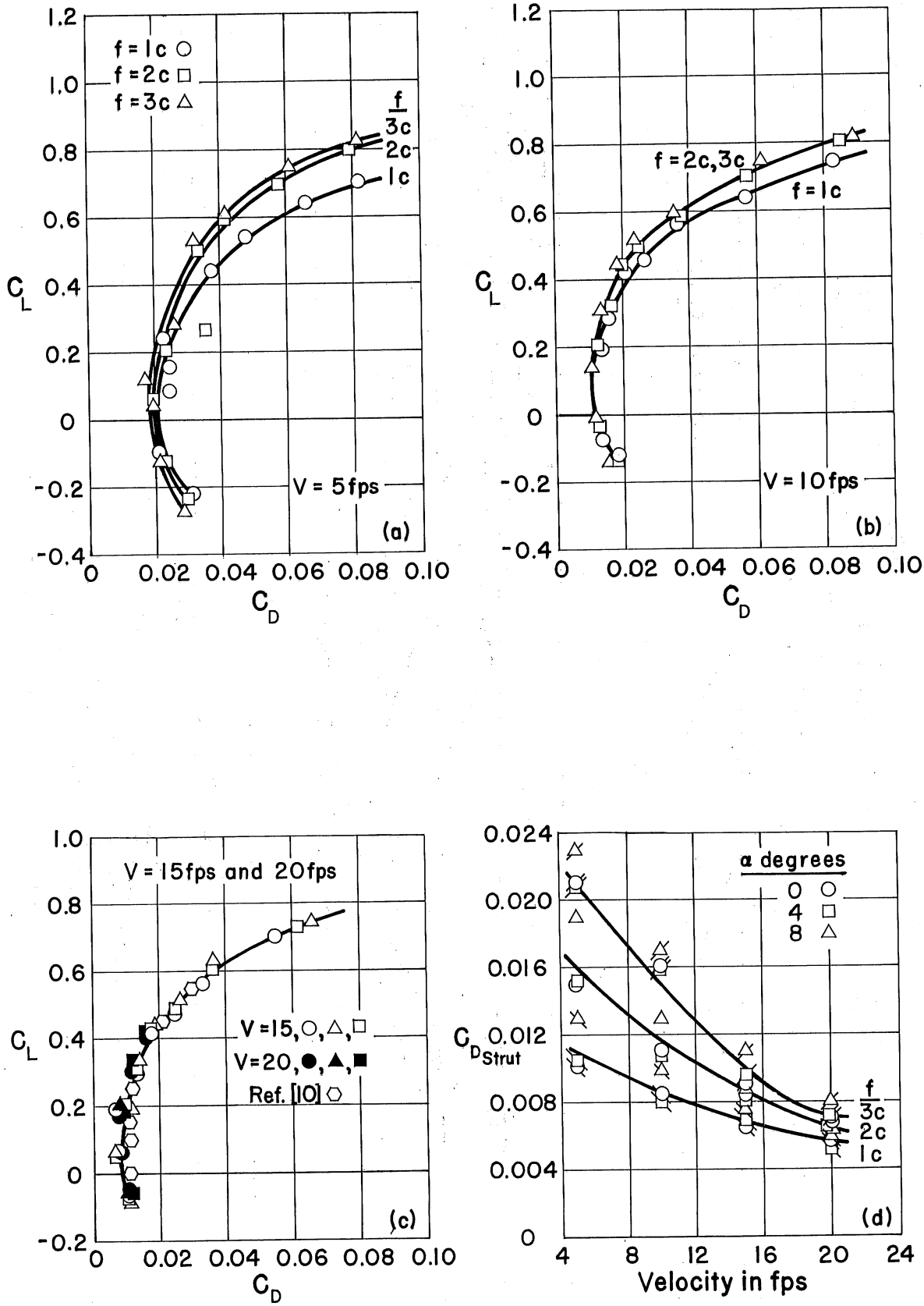

Fig. 3 - Polar Diagrams (Based on Net Drag) and Strut Drag--Smooth Water

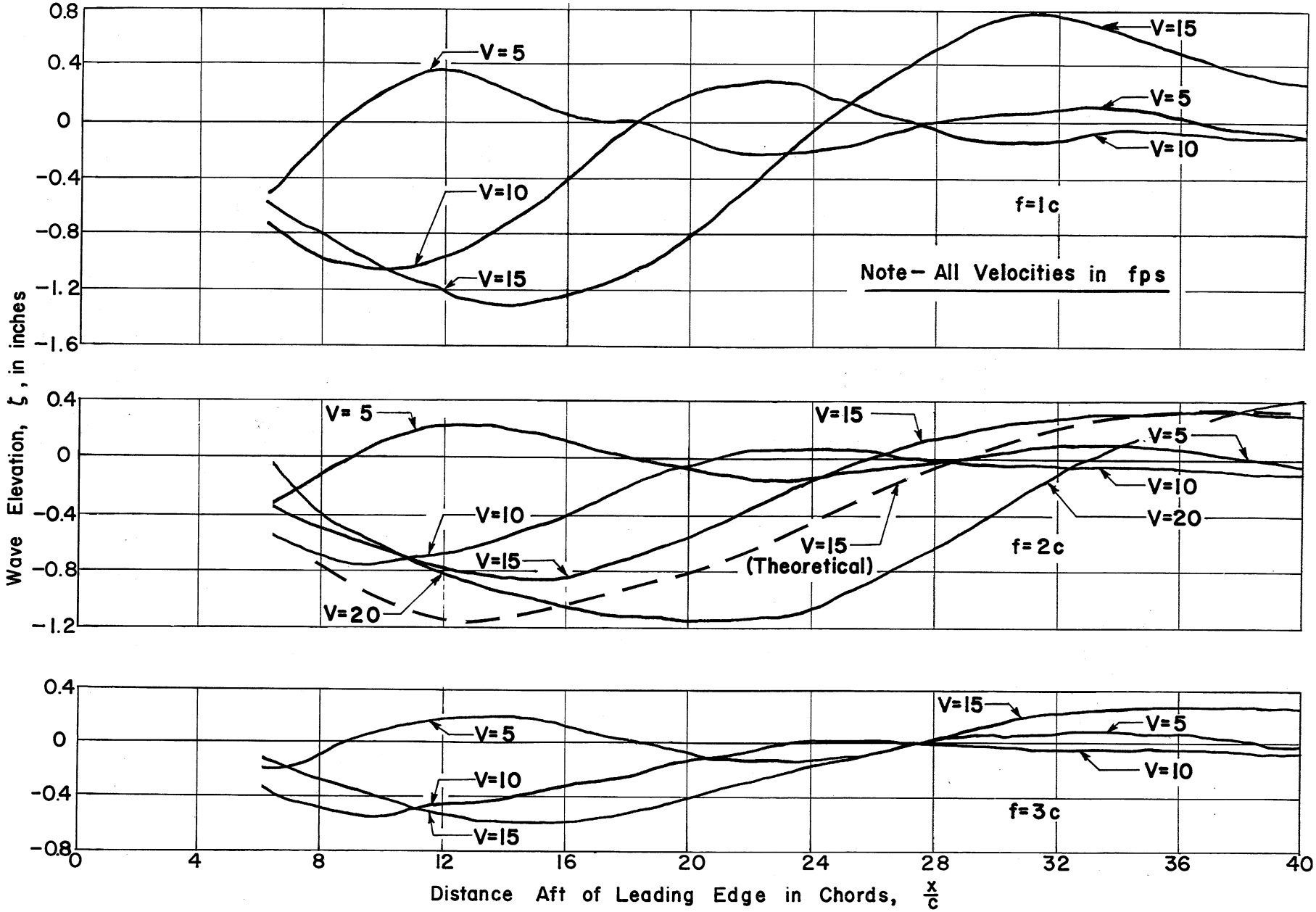

Fig. 4 – Longitudinal Wave Profiles at Centerspan, $\alpha = 4^{\circ}$

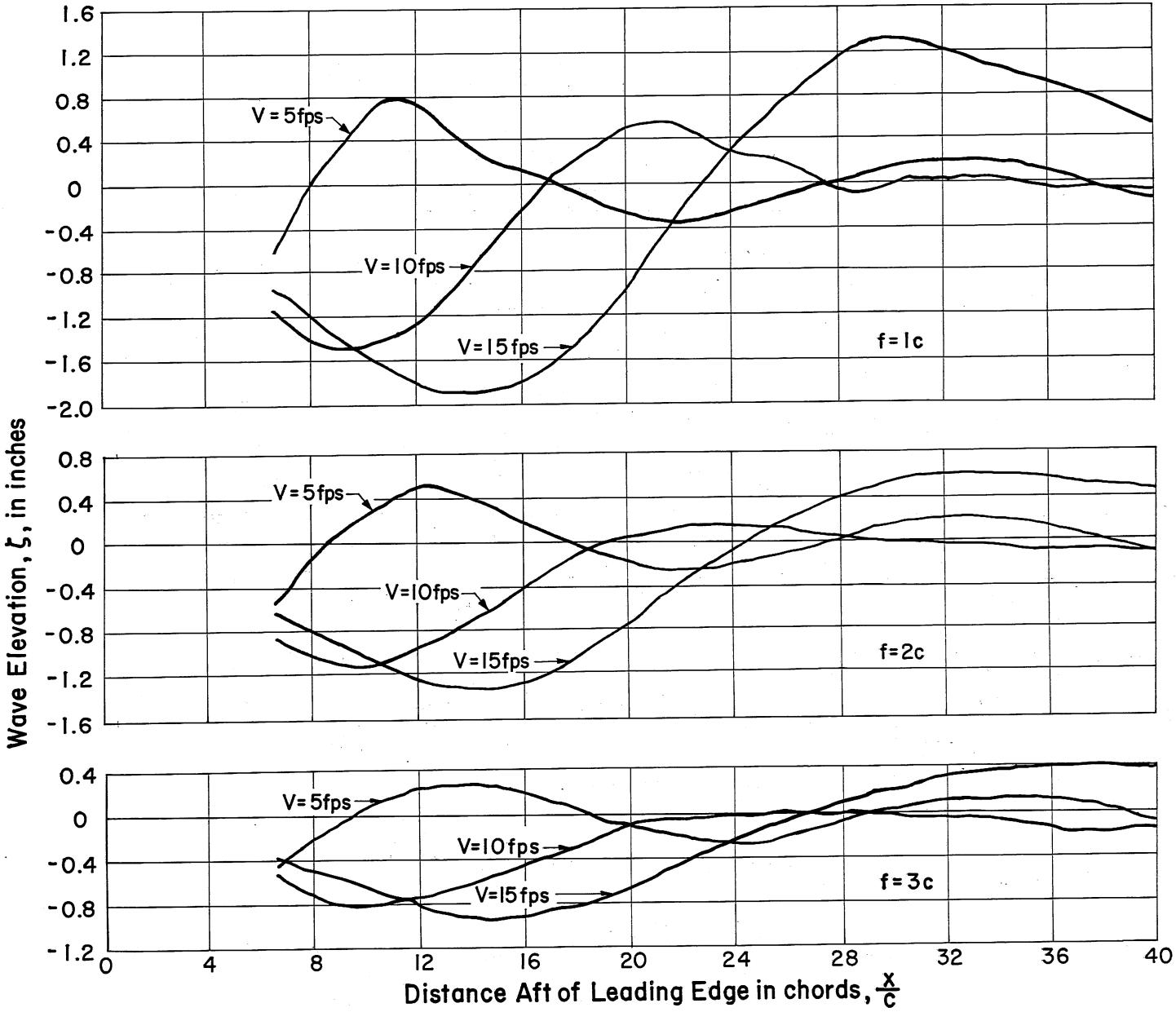

Fig. 5 – Longitudinal Wave Profiles at Centerspan, $\alpha = 8^{\circ}$

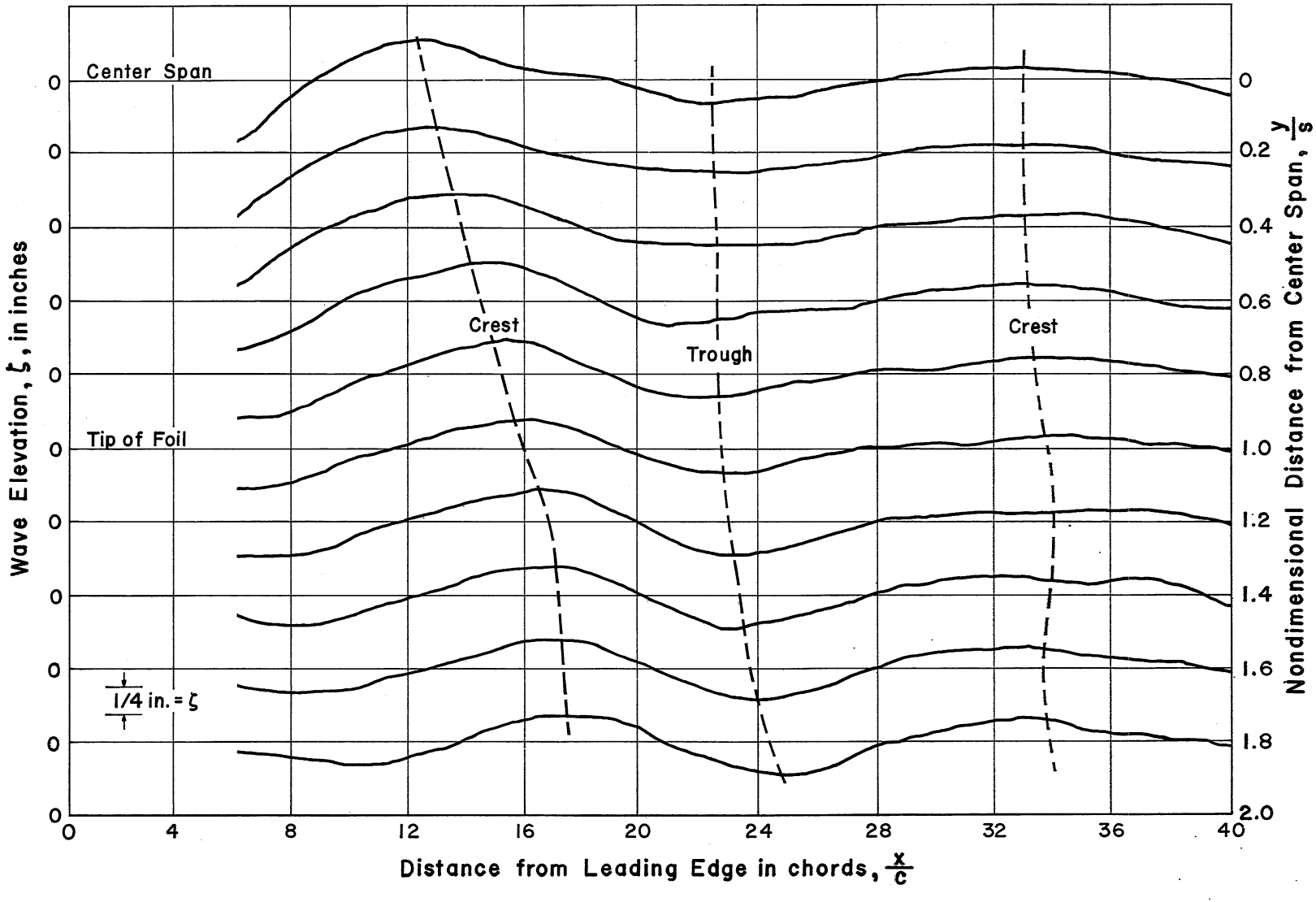

Fig. 6 - Longitudinal Wave Profiles at Various Spanwise Locations, $\alpha = 4^{o}$, f = 1 chord, V = 5 fps

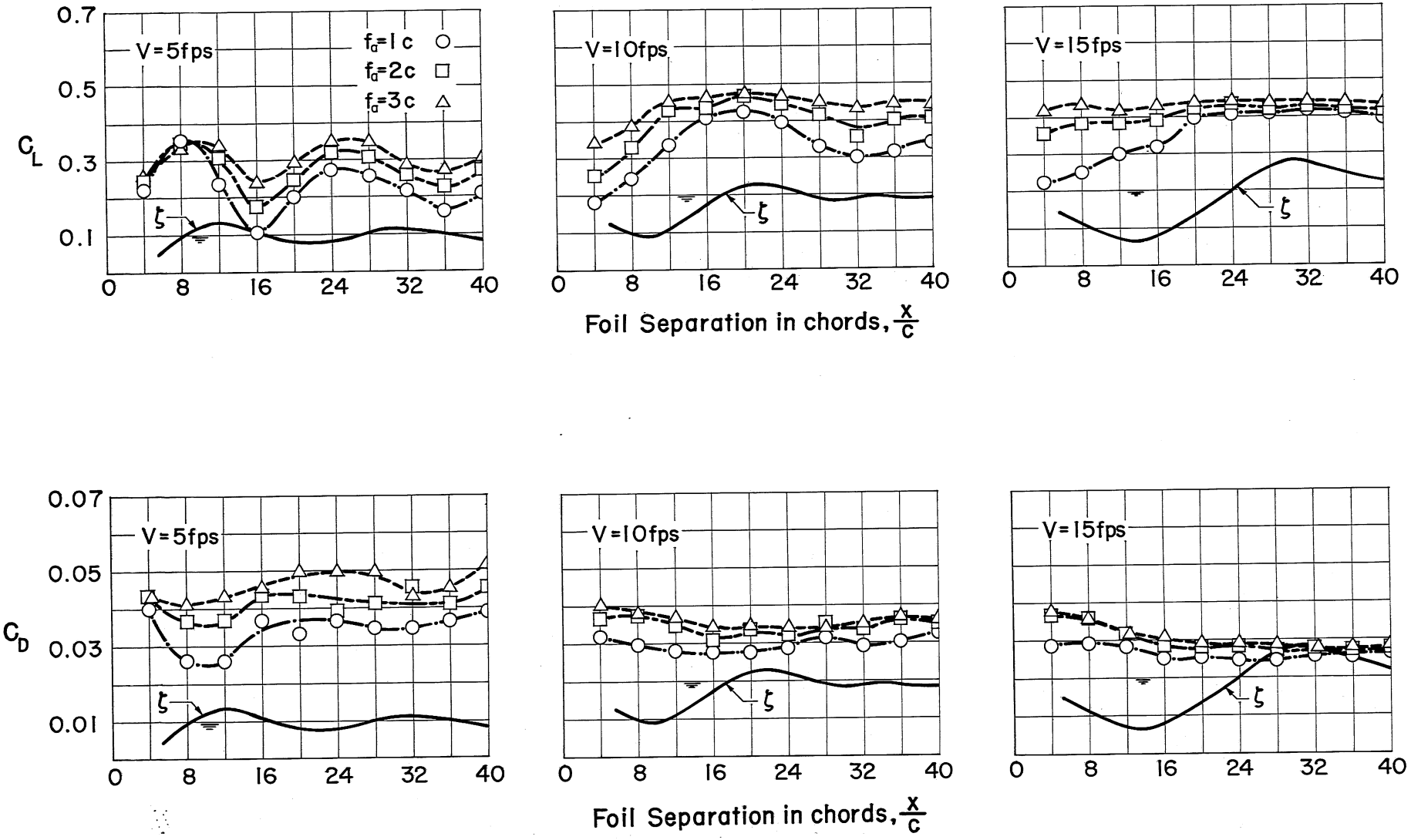

Fig. 7 – Force Coefficients for Aft Foil of Tandem Configuration, $\alpha_f = \alpha_a = 4^\circ$, f_f = 1 chord

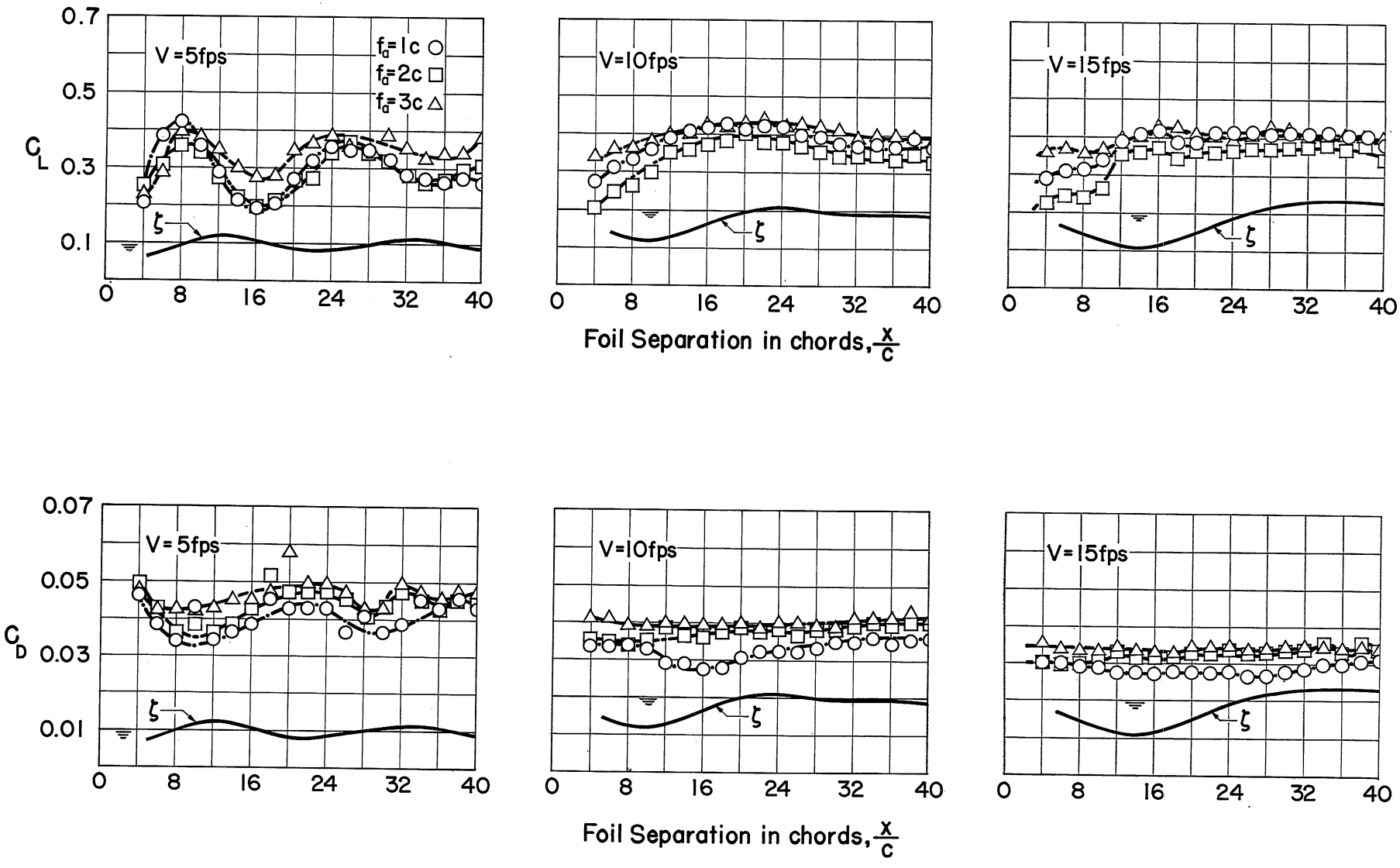

Fig. 8 - Force Coefficients for Aft Foil of Tandem Configuration, $\alpha_f = \alpha_a = 4^o$, $f_f = 2$ chords

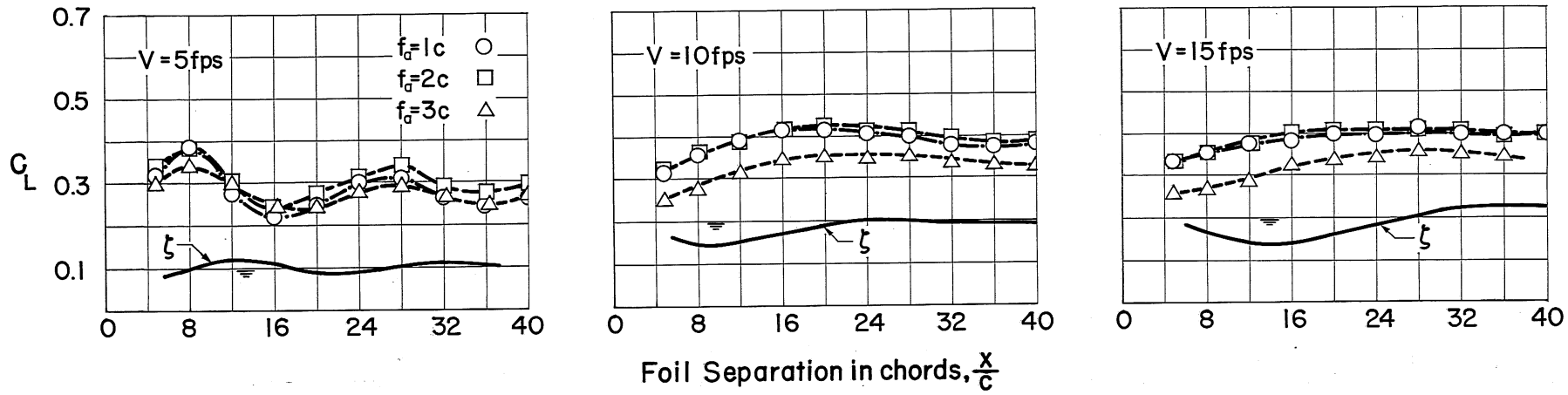

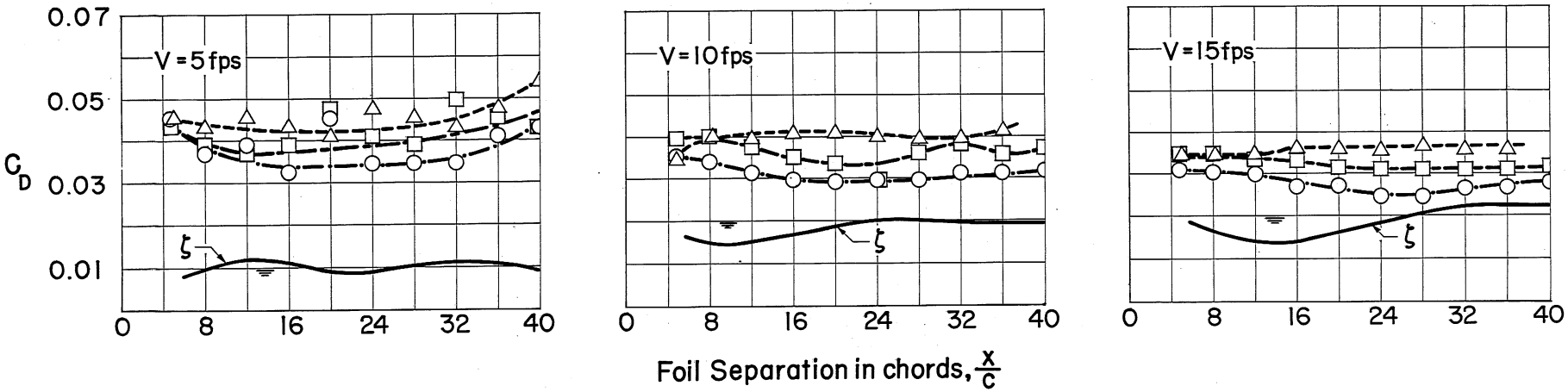

Fig. 9 – Force Coefficients for Aft Foil of Tandem Configuration,
$\alpha_f = \alpha_a = 4^o$, $f_f = 3$ chords

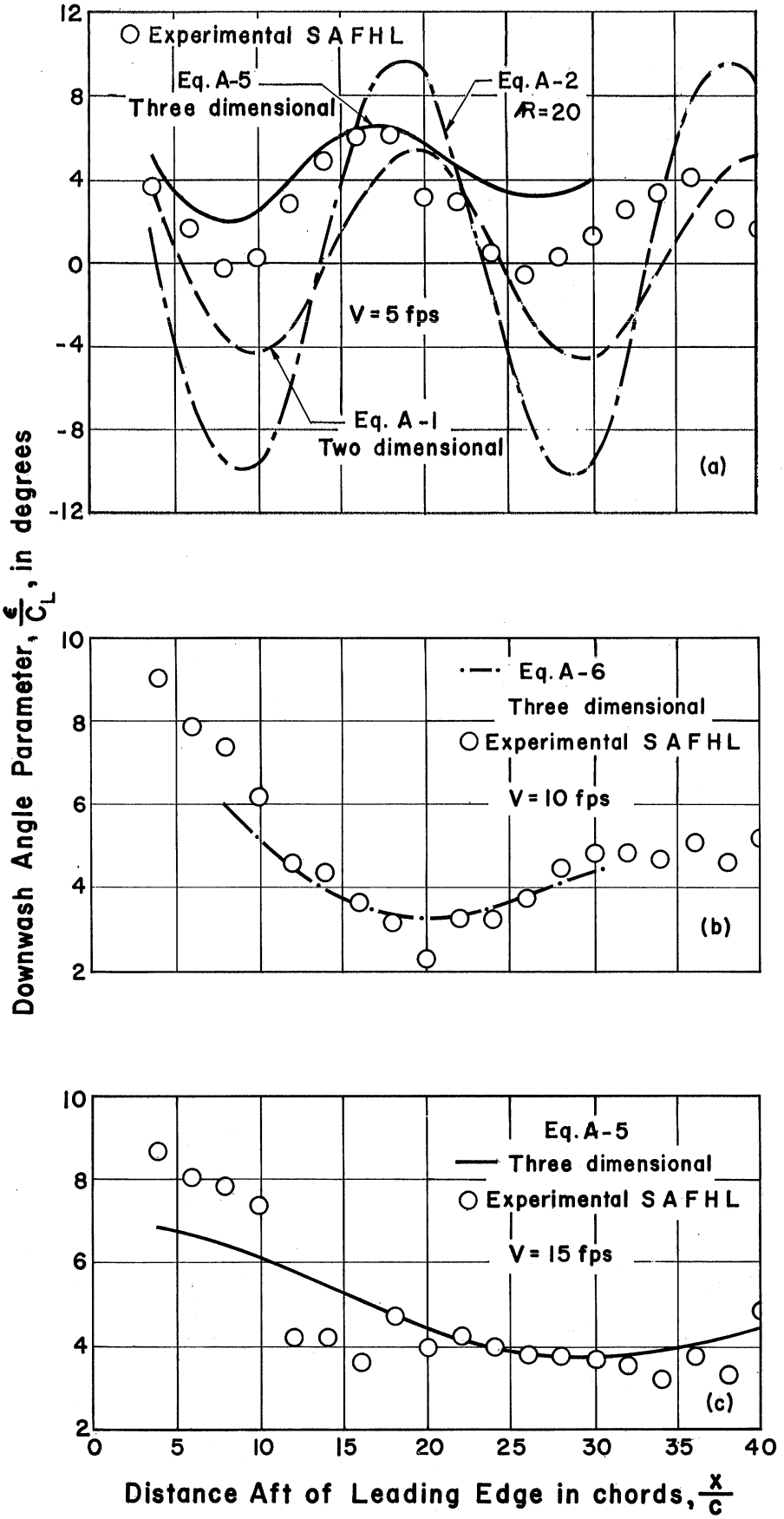

Fig. 10 - Comparison of Theoretical and Experimental Downwash Angles, $\alpha_f = \alpha_a = 4^o$, $f_f = f_a = 2$ chords

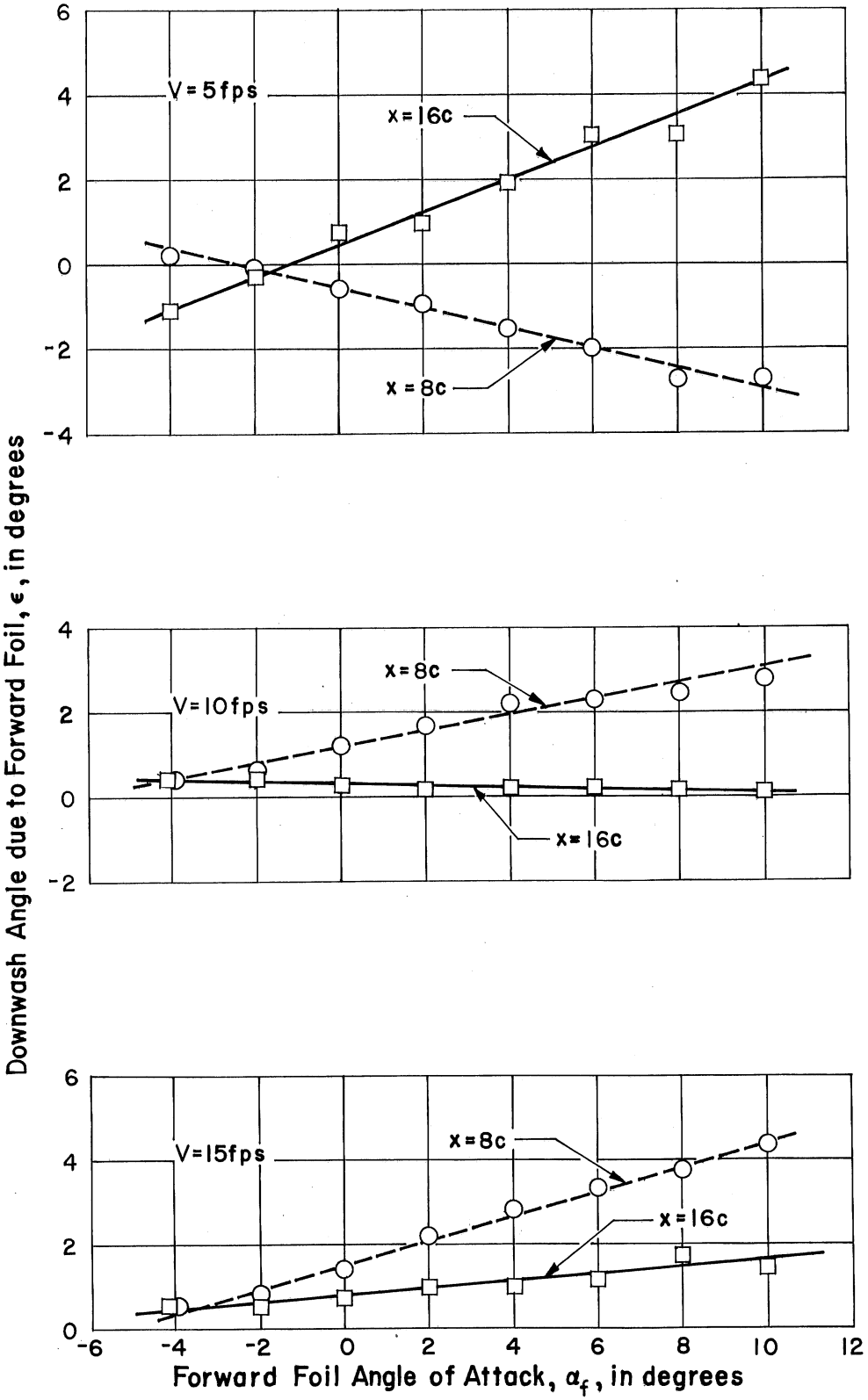

Fig. 11 – Variation of Downwash Angle with Angle of Attack, $\alpha_a = 4^\circ$, $f_f = f_a = 1$ chord

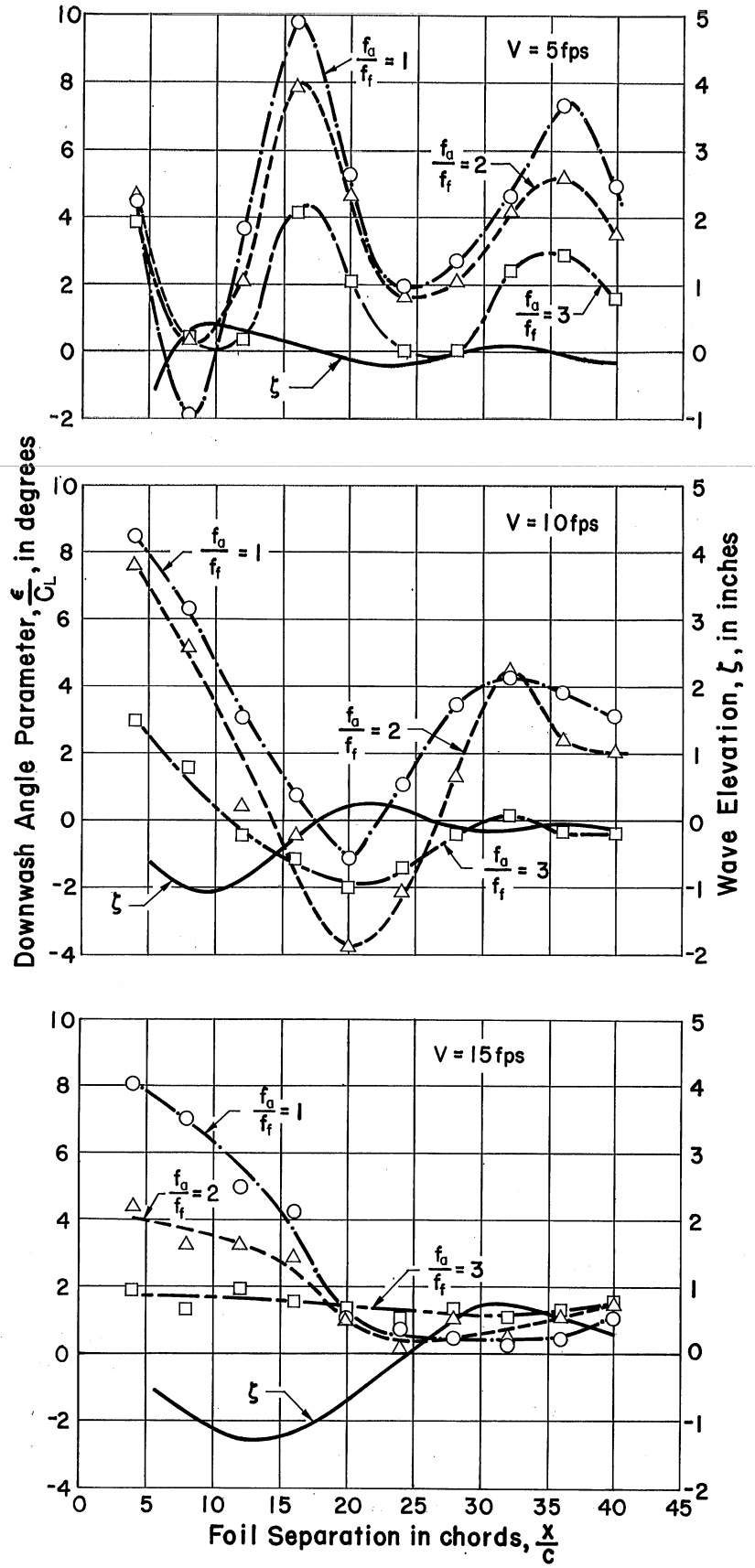

Fig. 12 – Variation of Downwash Angle with Foil Separation, $\alpha_f = \alpha_a = 4^\circ$, $f_f = 1$ chord

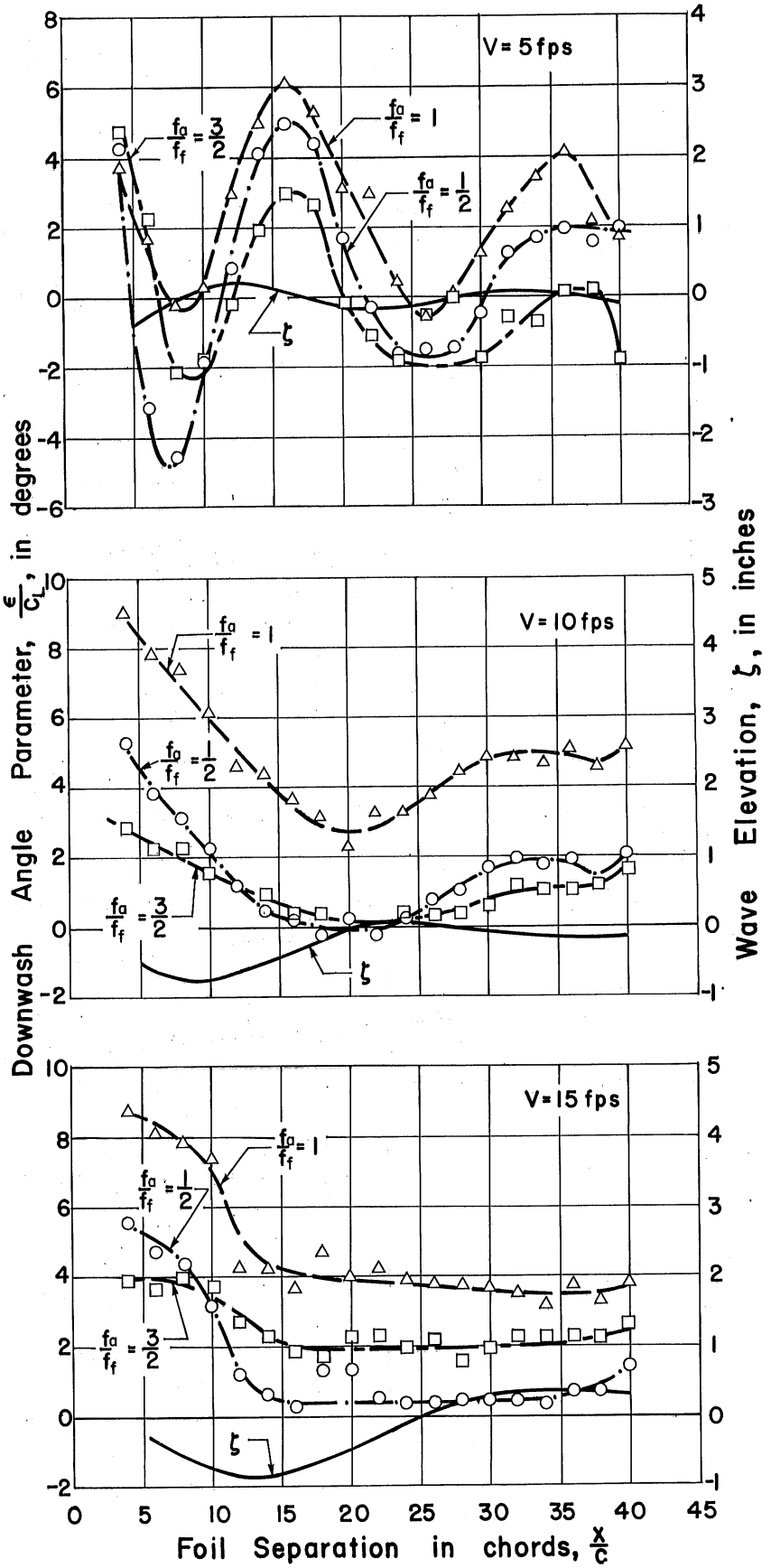

Fig. 13 – Variation of Downwash Angle with Foil Separation, $\alpha_f = \alpha_a = 4^o$, $f_f = 2$ chords

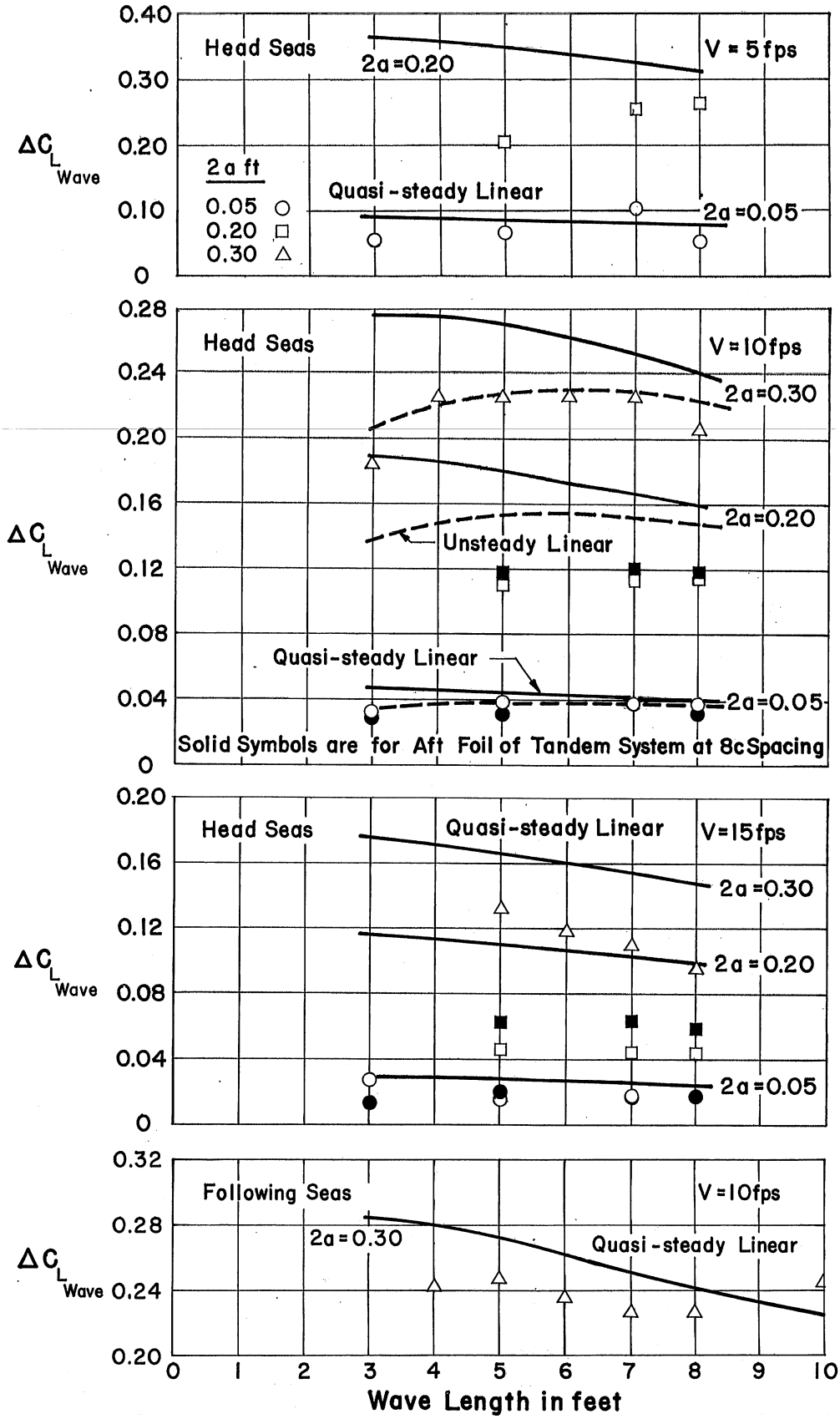

Fig. 14 – Additional Lift Coefficient due to Orbital Motion for a Single Foil Moving through a Progressive Wave Train, $\alpha = 4^{\circ}$, f = 1 chord

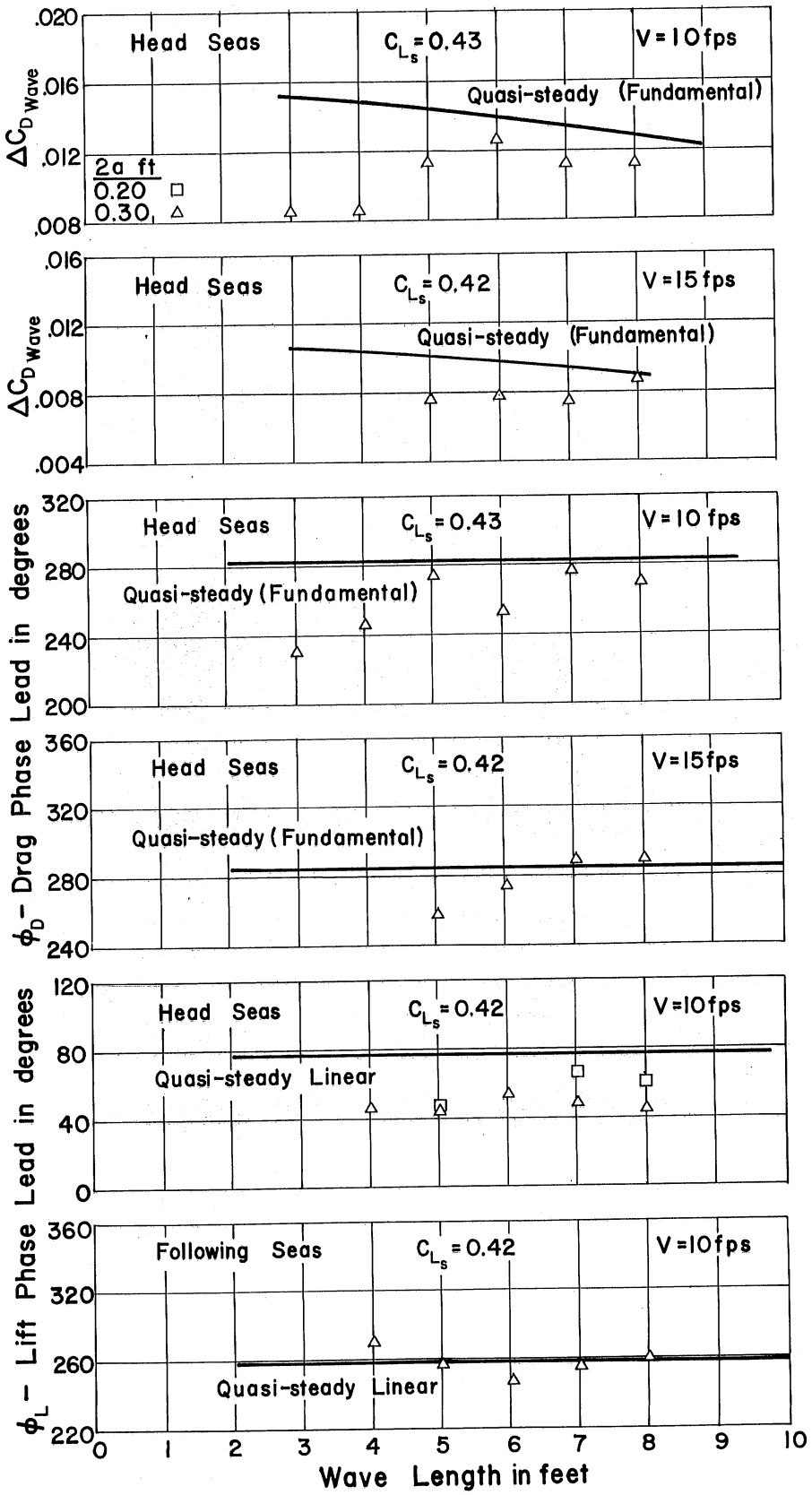

Fig. 15 - Additional Drag Coefficients and Phase Relationships for a Single Foil Moving through a Progressive Wave Train, $\alpha = 4^{\circ}$, f = 1 chord

A P P E N D I X

APPENDIX

The equations used for calculating the theoretical curves shown on several of the graphs are listed for reference purposes. Symbols not defined in the Appendix are given in the List of Symbols.

A. Two-Dimensional Formulae

1. Theoretical Development (Reference [2])

$$\frac{\epsilon}{C_L} = \frac{cx}{4\pi}\left[\frac{1}{x^2 + (y+f)^2} + \frac{1}{x^2 + (y-f)^2}\right] + K_o c e^{K_o(y-f)} \cos K_o x \qquad \text{(A-1)}$$

where x is the horizontal coordinate and y the vertical coordinate with the origin in the undisturbed free surface. K_o is a wave number equal to g/V^2.

The above expression is a first-order approximation taken from a development which assumes perturbations in the flow due to a hydrofoil represented by a single vortex and its image in the free surface, and satisfying the requisite boundary conditions. During the evaluation of the integrals involved, principal values are taken and nonoscillatory terms which attenuate rapidly with x are dropped. Hence the expression for ϵ/C_L is not accurate in the immediate vicinity of the foil.

2. Empirical Formula (Reference [11])

$$\frac{\epsilon}{C_L} = \frac{e^{-\frac{2}{F_f^2}}}{F_f^2} \cos\left(\frac{gx}{V^2} + 0.25\right) \qquad \text{(A-2)}$$

where $F_f = \dfrac{V}{\sqrt{gf}}$.

This empirical expression was based on experimental data from tests with a hydrofoil of aspect ratio 20 at a submergence of one chord. The downwash angles were evaluated at 15, 20, and 25 chords behind the foil. The data are shown in Fig. 24 of Reference [11].

B. Three-Dimensional Formulae

1. Limited Depth Theory (Reference [3])

For elliptical circulation distribution

$$\zeta = -\frac{4}{\pi} c C_L \int_{\theta_o}^{\pi/2} \frac{\sinh K(d-f).[K + K_o \sec^2\theta].e^{-Kd}.J_1(Ks \sin\theta).\sin(Kx \cos\theta).\cos(Ky \sin\theta)d\theta}{K_o(1 - Kod \sec^2\theta \operatorname{sech}^2 Kd) \sin\theta}$$

where $K = K_o \sec^2\theta \tanh Kd$,

d = water depth,

$\theta_o = 0$ for $\frac{V}{\sqrt{gd}} \leq 1$, and

$\theta_o = \cos^{-1}\left(\frac{\sqrt{gd}}{V}\right)$ for $\frac{V}{\sqrt{gd}} > 1.0$.

When d approaches infinity this reduces to the infinite depth theory of Reference [2]. For the test conditions at St. Anthony Falls Hydraulic Laboratory the results using the limited depth and infinite depth theories were not significantly different, the integrands becoming numerically identical for $\theta > \theta_o$. For $\theta < \theta_o$ the values of the integrand were zero in the case of the limited depth theory and very small in the case of the infinite depth theory.

2. Infinite Depth Theory (Reference [2])

$$\zeta = -\frac{4}{\pi} c C_L \int_0^{\pi/2} \left\{\sec^2\theta\, e^{-f K_o \sec^2\theta} \frac{\sin(K_o x \sec\theta) J_1(K_o s \sec^2\theta \sin\theta)\cos(K_o y \sec^2\theta \sin\theta)}{\sin\theta}\right\} d\theta \qquad \text{(A-4)}$$

The corresponding expression for the downwash angle in radians is

$$\frac{\epsilon}{C_L} = \frac{c}{\pi b s}\left\{b - \left[[(f+z)^2 + s^2 - b^2]^2 + 4(f+z)^2 b^2\right]^{1/4} \sin\beta'\right\}$$

$$- \frac{2c}{\pi b} \int_0^{\pi/2} e^{K_o(z-f)\sec^2\theta} \frac{\sec\theta\, J_1(K_o s \sec^2\theta \sin\theta)\sin(K_o b \sec^2\theta \sin\theta)d\theta}{\sin^2\theta}$$

$$+ \frac{4c}{\pi b} \int_0^{\pi/2} e^{K_o(z-f)\sec^2\theta} \frac{\sec\theta\, J_1(K_o s \sec^2\theta \sin\theta)\sin(K_o b \sec^2\theta \sin\theta)\cos(K_o x \sec\theta)d\theta}{\sin^2\theta}$$

At high speeds the second term in the expression for ϵ/C_L may be approximated by

$$-\frac{c}{\pi s}\left\{1-\frac{(f-z)/s}{[1+(\frac{f-z}{s})^2]^{1/2}}\right\} \qquad \text{(A-6)}$$

In Eq. (A-5)

$$\sin\beta' = \left\{1/2\left[1-\frac{(f+z)^2+s^2-b^2}{\sqrt{[(f+z)^2+s^2-b^2]^2+4(f+z)^2b^2}}\right]\right\}^{1/2}$$

The three-dimensional theory is taken from a development which represents the foil and its wake by a sheet of doublets whose width is equal to that of the foil. The potential is derived by differentiating the potential for a source in an infinite fluid, its image in the bottom, a correction potential which insures that free surface and bottom boundary conditions are satisfied, and a correction potential which eliminates waves ahead of the foil. Attention is again restricted to that part of the potential which is oscillatory so that the theory is not applicable in the immediate vicinity of the foil. Due to the neglect of certain terms in the evaluation of integrals occurring in the development it is expected that the theory will give poorest agreement with experimental data at low speeds. This is borne out by the St. Anthony Falls Hydraulic Laboratory results as shown in Fig. 10.

To allow some correction for the effect of roll-up of the tip vortices it is assumed that for the aft foil of a tandem system which has the same span as the forward foil, the average of the downwash will be close to the value at mid-span. It is further assumed that the correction commonly applied in classical airfoil theory for the variation of downwash along the longitudinal (x) axis in the plane of the foil may also be applied at any point not in the same horizontal plane as the foil. The theoretical evaluation and comparison of the downwash angle with experimental values are therefore made in the same horizontal plane as the forward foil since the theory would be expected to be more accurate in that plane. The difference between the expressions for ϵ/C_L given by Eqs. (A-5) and (A-6) was found to be small, even at 5 fps.

C. Foils Moving Through a Progressive Wave System

1. Quasi-Steady Equations

As indicated in the definition sketch, Fig. 1, the lift and drag axes are respectively perpendicular and parallel to the direction of motion. Thus, for a single foil restrained in heave and pitch moving through a regular wave represented by $\eta = a \sin \nu t$, the measured lift is

$$L = \frac{\rho}{2} S \left[(V - u)^2 + w^2\right] \left\{ C_L \cos \epsilon + C_D \sin \epsilon \right\} \qquad \text{(A-7)}$$

where $u = \mp a \frac{2\pi c_w}{\lambda} e^{-2\pi f/\lambda} \sin \nu t$,

$$w = \pm a \frac{2\pi c_w}{\lambda} e^{-2\pi f/\lambda} \cos \nu t,$$

$$\epsilon = \tan^{-1} \frac{w}{V - u},$$

$$\nu = \frac{2\pi}{\lambda} (V \pm c_w),$$

and the measured drag

$$D = \frac{\rho}{2} S \left[(V - u)^2 + w^2\right] \left\{ C_D \cos \epsilon - C_L \sin \epsilon \right\} \qquad \text{(A-8)}$$

In both equations, the upper sign is to be used for head seas, the lower sign for following seas.

By using quasi-steady assumptions for the lift and drag coefficients, the additional increment due to the waves can be written

$$C_L = C_{L_S} + \Delta C_{L_{wave}} = \sqrt{A^2 + B^2} \sin (\nu t + \phi_L) \qquad \text{(A-9)}$$

where $A = \pm a \frac{2\pi c_w}{\lambda V} e^{-2\pi f/\lambda} \left[C_{D_S} + \frac{\partial C_L}{\partial \alpha}\right]$,

$$B = \pm 2 C_{L_S} a \frac{2\pi c_w}{\lambda V} e^{-2\pi f/\lambda}, \text{ and}$$

$$\phi_L = \tan^{-1} A/B.$$

and

$$C_D - C_{D_S} = \Delta C_{D_{wave}} = \sqrt{A_1^2 + B_1^2}\ \sin(\nu t + \phi_{D_1}) + \sqrt{A_2^2 + B_2^2}\ \sin(2\nu t + \phi_{D_2}) + D$$

where $A_1 = \pm \frac{a 2\pi c_w}{\lambda V} e^{-2\pi f/\lambda}\ C_{L_S}\ [2 \frac{\partial C_D}{\partial C_L^2} \frac{\partial C_L}{\alpha} - 1]$,

$$B_1 = \pm 2\ C_{D_S} \frac{a 2\pi c_w}{\lambda V} e^{-2\pi f/V},$$

$$A_2 = \frac{[a \frac{2\pi c_w}{\lambda V} e^{-2\pi f/V}]^2}{2} [\frac{\partial C_D}{\partial C_L^2} (\frac{\partial C_L}{\partial \alpha})^2 - \frac{C_{D_S}}{2} - \frac{\partial C_L}{\partial \alpha}],$$

$$B_2 = \frac{[a \frac{2\pi c_w}{\lambda V} e^{-2\pi f/V}]^2}{2}\ C_{L_S}\ [2 \frac{\partial C_D}{\partial C_L^2} \frac{\partial C_L}{\partial \alpha} - 1],$$

$$D = [a \frac{2\pi c_w}{\lambda V} e^{-2\pi f/V}]^2\ [1/2 \frac{\partial C_D}{\partial C_L^2} (\frac{\partial C_L}{\partial \alpha})^2 - \frac{C_{D_S}}{4} - 1/2 \frac{\partial C_L}{\partial \alpha} + C_{D_S}],$$

$\phi_{D_1} = \tan^{-1} A_1/B_1$, and

$\phi_{D_2} = \tan^{-1} A_2/B_2$.

In the latter equation, terms up to the second power were retained, as the drag varies essentially as the square of the angle of attack. Inclusion of the horizontal component of velocity causes little change in the amplitude of the forces, but has greater effect on the phase relationship. If the horizontal component of velocity is neglected in the lift expression, the lift would lead the wave by 90 degrees. In the case of the drag, the drag would lag the wave by 90 degrees, or be 180 degrees out of phase with the lift.

Also, if the amplitude of the wave is small, it is possible to neglect the term in Eq. (A-10) containing the second harmonic with little error. However, for a wave of 4-ft length and 0.15-ft amplitude and a towing velocity

of 10 fps in head seas, the amplitude of the second harmonic may be 50 per cent of the fundamental.

2. Unsteady Equations.

Computations for the unsteady lift were carried out from equations developed by Kaplan and presented in Reference [12]. Neglecting the second harmonic component, the additional lift for a foil moving through head seas is given by

$$\Delta L_{wave} = \pm \mathrm{Re} \left\{ \frac{\rho \pi S V^2}{1 + 2/AR} \frac{a 2\pi c_w}{\lambda V} e^{-2\pi f/\lambda} (1 - i\alpha_s) e^{i\nu t} \right.$$

$$\left. \left(\left[J_o\left(\frac{\pi c}{\lambda}\right) - i J_1 \left(\frac{\pi c}{\lambda}\right) \right] C\left(\frac{\nu c}{2V}\right) + i \left(1 \pm \frac{c_w}{V}\right) J_1\left(\frac{\pi c}{\lambda}\right) \right) \right\} \qquad \text{(A-11)}$$

where J_o and J_1 = Bessel functions of first kind, orders zero and one,

$C\left(\frac{\nu V}{2V}\right)$ = Theodorsen's function with argument $\frac{\nu c}{2V}$, and

α_s = angle of attack for foil in smooth water.

SPONSOR'S DISTRIBUTION LIST FOR PROJECT REPORT NO. 61

of the St. Anthony Falls Hydraulic Laboratory

Copies	Organization
6	Chief of Naval Research, Department of the Navy, Washington 25, D. C., Attn: 3 - Code 438 1 - Code 461 1 - Code 463 1 - Code 466
1	Commanding Officer, Office of Naval Research Branch Office, 495 Summer Street, Boston 10, Massachusetts.
1	Commanding Officer, Office of Naval Research Branch Office, 207 West 24th Street, New York 11, New York.
1	Commanding Officer, Office of Naval Research Branch Office, 1030 East Green Street, Pasadena, California.
1	Commanding Officer, Office of Naval Research Branch Office, 1000 Geary Street, San Francisco 9, California.
25	Commanding Officer, Office of Naval Research Branch Office, Navy 100, Fleet Post Office, New York, New York.
6	Director, Naval Research Laboratory, Washington 25, D. C., Attn: Code 2027.
5	Chief, Bureau of Naval Weapons, Department of the Navy, Washington 25, D. C., Attn: 1 - Code RUAW-4 1 - Code RRRE 1 - Code RAAD 1 - Code RAAD-222 1 - Code DIS-42
8	Chief, Bureau of Ships, Department of the Navy, Washington 25, D. C., Attn: 1 - Code 310 1 - Code 312 1 - Code 335 1 - Code 420 1 - Code 421 1 - Code 440 1 - Code 442 1 - Code 449
1	Chief, Bureau of Yards and Docks, Department of the Navy, Washington 25, D. C., Attn: Code D-400.

Copies	Organization
15	Commanding Officer and Director, David Taylor Model Basin, Washington 7, D. C., Attn: 1 - Code 108 1 - Code 142 1 - Code 500 1 - Code 513 1 - Code 520 1 - Code 526 1 - Code 526A 1 - Code 530 1 - Code 533 1 - Code 580 1 - Code 585 1 - Code 589 1 - Code 591 1 - Code 591A 1 - Code 700
1	Commander, U. S. Naval Ordnance Test Station, China Lake, California, Attn: Code 753.
1	Commander, U. S. Naval Ordnance Test Station, Pasadena Annex, 3202 E. Foothill Blvd., Pasadena 8, California, Attn: Code P-508.
1	Commander, Planning Department, Portsmouth Naval Shipyard, Portsmouth, New Hampshire.
1	Commander, Planning Department, Boston Naval Shipyard, Boston 29, Massachusetts.
1	Commander, Planning Department, San Francisco Naval Shipyard, San Francisco 24, California.
1	Commander, Planning Department, Pearl Harbor Naval Shipyard, Navy 128, Fleet Post Office, San Francisco, California.
1	Commander, Planning Department, Mare Island Naval Shipyard, Vallejo, California.
1	Commander, Planning Department, New York Naval Shipyard, Brooklyn 1, New York.
1	Commander, Planning Department, Puget Sound Naval Shipyard, Bremerton, Washington.
1	Commander, Planning Department, Philadelphia Naval Shipyard, U. S. Naval Base, Philadelphia 12, Pennsylvania.
1	Commander, Planning Department, Norfolk Naval Shipyard, Portsmouth, Virginia.
1	Commander, Planning Department, Charleston Naval Shipyard, U. S. Naval Base, Charleston, South Carolina.

Copies	Organization
1	Commander, Planning Department, Long Beach Naval Shipyard, Long Beach 2, California.
1	Commander, Planning Department, U. S. Naval Weapons Laboratory, Dahlgren, Virginia.
1	Commander, U. S. Naval Ordnance Laboratory, White Oak, Maryland.
1	Dr. A. V. Hershey, Computation and Exterior Ballistics Laboratory, U. S. Naval Weapons Laboratory, Dahlgren, Virginia.
1	Superintendent, U. S. Naval Academy, Annapolis, Maryland, Attn: Library.
1	Superintendent, U. S. Naval Postgraduate School, Monterey, California.
1	Commandant, U. S. Coast Guard, 1300 E Street, N. W., Washington D. C.
1	Secretary Ship Structure Committee, U. S. Coast Guard Headquarters, 1300 E Street, N. W., Washington, D. C.
1	Commander, Military Sea Transportation Service, Department of the Navy, Washington 25, D. C.
3	U. S. Maritime Administration, GAO Building, 441 G Street, N. W., Washington, D. C., Attn: 1 - Division of Ship Design 1 - Division of Research 1 - Mr. R. P. Godwin
1	Superintendent, U. S. Merchant Marine Academy, Kings Point, Long Island, New York, Attn: Capt. L. S. McCready (Dept. of Engineering)
1	Commanding Officer and Director, U. S. Navy Mine Defense Laboratory, Panama City, Florida.
1	Commanding Officer, NROTC and Naval Administrative Unit, Massachusetts Institute of Technology, Cambridge 39, Massachusetts.
2	U. S. Army Transportation Research and Development Command, Fort Eustis, Virginia, Attn: Marine Transport Division.
1	Director of Research, National Aeronautics and Space Administration, 1512 H Street, N. W., Washington 25, D. C.
4	Director, Langley Research Center, Langley Field, Virginia, Attn: 2 - Mr. J. B. Parkinson 1 - Mr. I. E. Garrick 1 - Mr. D. J. Marten
1	Director Engineering Sciences Division, National Science Foundation, 1951 Constitution Avenue, N. W., Washington 25, D. C.

Copies	Organization
3	Director, National Bureau of Standards, Washington 25, D. C., Attn: 1 - Fluid Mechanics Division (Dr. G. B. Schubauer) 1 - Dr. G. H. Keulegan 1 - Dr. J. M. Franklin
10	Armed Services Technical Information Agency, Arlington Hall Station, Arlington 12, Virginia.
1	Office of Technical Services, Department of Commerce, Washington 25, D. C.
3	California Institute of Technology, Pasadena 4, California, Attn: 1 - Professor M. S. Plesset 1 - Professor T. Y. Wu 1 - Professor A. J. Acosta
1	University of California, Department of Engineering, Los Angeles 24, California, Attn: Dr. A. Powell.
1	Director, Scripps Institute of Oceanography, University of California, La Jolla, California.
1	Professor M. L. Albertson, Department of Civil Engineering, Colorado A and M College, Fort Collins, Colorado.
1	Professor J. E. Cermak, Department of Civil Engineering, Colorado State University, Fort Collins, Colorado.
1	Professor W. R. Sears, Graduate School of Aeronautical Engineering, Cornell University, Ithaca, New York.
2	State University of Iowa, Iowa Institute of Hydraulic Research, Iowa City, Iowa, Attn: 1 - Dr. H. Rouse 1 - Dr. L. Landweber
2	Harvard University, Cambridge 38, Massachusetts, Attn: 1 - Professor G. Birkhoff (Dept. of Mathematics) 1 - Professor G. F. Carrier (Dept. of Mathematics)
2	Massachusetts Institute of Technology, Cambridge 39, Massachusetts, Attn: 1 - Department of Naval Architecture and Marine Engineering 1 - Professor A. T. Ippen
3	University of Michigan, Ann Arbor, Michigan, Attn: 1 - Professor R. B. Couch (Dept. of Naval Architecture) 1 - Professor W. W. Willmarth (Aero. Engrg. Department) 1 - Professor M. S. Uberoi (Aero. Engrg. Department)
3	Dr. L. G. Straub, Director, St. Anthony Falls Hydraulic Laboratory, University of Minnesota, Minneapolis 14, Minnesota, Attn: 1 - Mr. J. M. Wetzel 1 - Mr. E. Silberman

Copies	Organization
1	Professor J. J. Foody, Engineering Department, New York State University Maritime College, Fort Schulyer, New York.
3	New York University, Institute of Mathematical Sciences, 25 Waverly Place, New York 3, New York, Attn: 1 - Professor J. Keller 1 - Professor J. J. Stoker 1 - Professor R. Kraichman
3	The Johns Hopkins University, Department of Mechanical Engineering, Baltimore 18, Maryland, Attn: 1 - Professor S. Corrsin 2 - Professor O. M. Phillips
1	Massachusetts Institute of Technology, Department of Naval Architecture and Marine Engineering, Cambridge 39, Massachusetts, Attn: Prof. M. A. Abkowitz, Head.
2	Dr. G. F. Wislicenus, Ordnance Research Laboratory, Pennsylvania State University, University Park, Pennsylvania, Attn: Dr. M. Sevik.
1	Professor R. C. Diprima, Department of Mathematics, Rensselaer Polytechnic Institute, Troy, New York.
5	Stevens Institute of Technology, Davidson Laboratory, Castle Point Station, Hoboken, New Jersey, Attn: 1 - Professor E. V. Lewis 1 - Mr. D. Savitsky 1 - Mr. J. P. Breslin 1 - Mr. C. J. Henry 1 - Mr. S. Tsakonas
1	Webb Institute of Naval Architecture, Crescent Beach Road, Glen Cove, New York, Attn: Technical Library.
1	Director, Woods Hole Oceanographic Institute, Woods Hole, Massachusetts.
1	Executive Director, Air Force Office of Scientific Research, Washington 25, D. C., Attn: Mechanics Branch.
1	Commander, Wright Air Development Division, Aircraft Laboratory, Wright-Patterson Air Force Base, Ohio, Attn: Mr. W. Mykytow, Dynamics Branch.
2	Cornell Aeronautical Laboratory, 4455 Genesee Street, Buffalo, New York, Attn: 1 - Mr. W. Targoff 1 - Mr. R. White

Copies	Organization
3	Massachusetts Institute of Technology, Fluid Dynamics Research Laboratory, Cambridge 39, Massachusetts, Attn: 1 - Professor H. Ashley 1 - Professor M. Landahl 1 - Professor J. Dugundji
2	Hamburgische Schiffbau-Versuchsanstalt, Bramfelder Strasse 164, Hamburg 33, Germany, Attn: 1 - Dr. O. Grim 1 - Dr. H. W. Lerbs
1	Institut für Schiffbau der Universität Hamburg, Berliner Tor 21, Hamburg 1, Germany, Attn: Professor G. P. Weinblum, Director.
1	Max-Planck Institut für Strömungsforschung, Bottingerstrasse 6/8, Gottingen, Germany, Attn: Dr. H. Reichardt.
1	Hydro-og Aerodynamisk Laboratorium, Lyngby, Denmark, Attn: Professor Carl Prohaska.
1	Skipsmodelltanken, Trondheim, Norway, Attn: Professor J. K. Lunde.
3	Versuchsanstalt für Wasserbau und Schiffbau, Schleuseninsel im Tiergarten, Berlin, Germany, Attn: 1 - Dr. S. Schuster, Director 1 - Dr. Grosse 1 - Dr. H. Schwanecke
1	Technische Hogeschool, Institut voor Toegepaste Wiskunde, Julianalaan 132, Delft, Netherlands, Attn: Professor R. Timman.
1	Bureau d'Analyse et de Recherche Appliquees, 47 Avenue Victor Cresson, Issy les Moulineaux Seine, Paris, France, Attn: Prof. Seistrunck.
1	Netherlands Ship Model Basin, Wageningen, Netherlands, Attn: Dr. Ir. J. D. van Manen.
1	Allied Research Associates, Inc., 43 Leon Street, Boston 15, Massachusetts, Attn: Dr. T. R. Goodman
2	National Physical Laboratory, Teddington, Middlesex, England, Attn: 1 - Mr. A. Silverleaf, Superintendent Ship Division 1 - Head Aerodynamics Division
2	Head, Aerodynamics Department, Royal Aircraft Establishment, Farnborough, Hants, England, Attn: Mr. M. O. W. Wolfe.
1	Boeing Airplane Company, Seattle Division, Seattle, Washington, Attn: Mr. M. J. Turner.
1	The Boeing Company, Aero-Space Division, Seattle 24, Washington, Attn: Mr. R. E. Bateman (Internal Mail Section 46-74).

Copies	Organization
1	Electric Boat Division, General Dynamics Corporation, Groton, Connecticut, Attn: Mr. Robert McCandliss.
1	General Applied Sciences Labs, Inc., Merrick and Stewart Avenues, Westbury, Long Island, New York.
1	Gibbs and Cox, Inc., 21 West Street, New York, New York.
3	Grumman Aircraft Engineering Corp., Bethpage, Long Island, New York, Attn: 1 - Mr. E. Baird 1 - Mr. E. Bower 1 - Mr. W. P. Carl
1	Lockheed Aircraft Corporation, Missiles and Space Division, Palo Alto, California, Attn: R. W. Kermeen.
1	Midwest Research Institute, 425 Volker Blvd., Kansas City 10, Missouri, Attn: Mr. Zeydel.
3	Director, Department of Mechanical Sciences, Southwest Research Institute, 8500 Culebra Road, San Antonio 6, Texas, Attn: 1 - Dr. H. N. Abramson 1 - Mr. G. Ransleben 1 - Editor, Applied Mechanics Reviews
2	Convair, A Division of General Dynamics, San Diego, California, Attn: 1 - Mr. R. H. Oversmith 1 - Mr. H. T. Brooke
1	Dr. S. F. Hoerner, 148 Busteed Drive, Midland Park, New Jersey.
1	Hydronautics, Incorporated, 200 Monroe Street, Rockville, Maryland. Attn: Mr. Phillip Eisenberg.
1	Rand Development Corporation, 13600 Deise Avenue, Cleveland 10, Ohio, Attn: Dr. A. S. Iberall.
1	U. S. Rubber Company, Research and Development Department, Wayne, New Jersey, Attn: Mr. L. M. White.
1	Technical Research Group, Inc., 2 Aerial Way, Syosset, Long Island, New York, Attn: Mr. Jack Kotik.
1	Mr. C. Wigley, Flat 102, 6-9 Charterhouse Square, London, E. C. 1, England.
1	AVCO Corporation, Lycoming Division, 1701 K Street, N. W., Apt. No. 904, Washington, D. C., Attn: Mr. T. A. Duncan.
1	Mr. J.G. Baker, Baker Manufacturing Company, Evansville, Wisconsin.

Copies	Organization
1	Curtiss-Wright Corporation Research Division, Turbomachinery Division, Quehanna, Pennsylvania, Attn: Mr. George H. Pedersen.
1	Dr. Blaine R. Parkin, AiResearchManufacturing Corporation, 9851-9951 Sepulveda Boulevard, Los Angeles 45, California.
1	National Research Council, Montreal Road, Ottawa 2, Canada, Attn: Mr. E. S. Turner.
1	The Rand Corporation, 1700 Main Street, Santa Monica, California, Attn: Technical Library.
2	StanfordUniversity, Department ofCivil Engineering, Stanford, California, Attn: 1 - Dr. Byrne Perry 1 - Dr. E. Y. Hsu
1	Waste King Corporation, 5550 Harbor Street, Los Angeles 22, California, Attn: Dr. A. Schneider.
1	Mr. David Wellinger, Hydrofoil Projects, Radio Corporation of America, Burlington, Massachusetts.
1	Hydrofoil Corporation of America, P. O. Box 11055, San Diego 11, California, Attn: Mr. John Bader, President.
1	Dr. Hirsch Cohen, IBMResearch Center, P. O. Box 218, Yorktown Heights, New York.
1	Food Machinery Corporation, P. O. Box 367, San Jose, California, Attn: Mr. G. Tedrew.